

# Adaptive Learning with Blockwise Missing and Semi-Supervised Data

Yiming Li<sup>1</sup>, Ying Wei<sup>1</sup> and Molei Liu<sup>2,3</sup>

1. Department of Biostatistics, Columbia University

2. Department of Biostatistics, Peking University

3. Beijing International Center for Mathematical Research, Peking University

## Abstract

Data fusion enables powerful and generalizable analyses across multiple sources. However, different data collection capacities across different sources lead to blockwise missingness (BM), which poses challenges in practice. Meanwhile, the high cost of obtaining gold-standard labels leaves the majority of samples unlabeled, known as the semi-supervised (SS) problem. In this paper, we propose a novel **D**ata-adaptive **E**stimation approach for data **F**Uision in the **S**Emi-supervised setting (DEFUSE) that handles both BM and SS issues in the presence of distributional shifts across data sources under a missing at random (MAR) mechanism. DEFUSE starts with a complete-data-only estimator derived from the primary data source, and uses data-adaptive and distributional-shift-adjusted procedures to successively incorporate the data with BM covariates and the large unlabeled sample to effectively reduce the estimation variance without incurring bias. To further avoid bias due to fusion of misaligned data violating of the MAR assumption, a screening method is developed to identify and exclude data sources that are not aligned with the primary source. Compared to existing approaches, DEFUSE offers two main improvements. First, it offers a new data-adaptive control variate approach to handle BM, which achieves intrinsic efficiency and robustness against distributional shifts. Second, it reveals a more essential role for the unlabeled sample in the BM regression problem, leading to improved estimation. These advantages are theoretically guaranteed and empirically supported by simulation studies and two real-world biomedical applications.

*Keywords:* Data fusion; Distributional shift; Missing at random; Control variate; Intrinsic efficiency.

## 1 Introduction

### 1.1 Background

Data fusion is the process of integrating multiple data sources to obtain richer and more comprehensive insights than what could be achieved by analyzing each source separately.

It has been increasingly used in many applications. For example, in the field of health and medicine, there has been growing interest and effort in linking electronic medical records (EMRs) with biobank data to tackle complex health issues (e.g., Castro et al., 2022). EMRs include detailed longitudinal clinical observations of patients, offering a rich source of health information over time. By combining these records with multi-omics data from biobanks, this type of data fusion allows for a much deeper understanding of disease prognosis at the molecular level, potentially transforming patient care and treatment strategies (e.g., Zengini et al., 2018). Beyond integrating different types of data, data fusion has also been scaled up to merge data from multiple institutions. The All-of-Us Research Program (The All of Us Research Program Investigators, 2019) is a prime example.

To effectively analyze fused datasets, particularly those combined with EMR, several major statistical challenges must be addressed. *Distributional shift* across data sources has been frequently studied in the past years (e.g., Gretton et al., 2009). Beyond this challenge, structural heterogeneity of multi-source data sets can severely impede data fusion. One specific common issue is known as *blockwise missingness* (BM) of covariates, which arises when variables are collected or defined differently across sources, resulting in one or multiple blocks of missing data in the merged data. Additionally, EMR-related research often suffers from incomplete or unreliable outcome labels. Obtaining accurate labels requires extensive manual review by clinical experts or long-term follow-up with patients. That leaves many patient outcomes unobserved/unlabeled in EMR. In such cases, *semi-supervised* (SS) learning is particularly valuable, as it combines a small subset of accurately labeled data with a large unlabeled sample from the same population. In situations where EMR data is linked with other data resources, the issues of BM and SS often occur simultaneously; see the real-world case study in Section 5. This new setup involves a more complex data structure, which we formally describe in Section 1.2. The complexity of EMR-fused data motivates our methodological development.

## 1.2 Problem Setup

Let  $Y$  be the outcome of interest and let  $\mathbf{X} = (X_1, X_2, \dots, X_p)^\top$  denote a  $p$ -dimensional vector of covariates. There are three types of data structures in a fused data. (i) **Labeled**

**Complete ( $\mathcal{LC}$ )** data source, which consists of labeled and complete observations. (ii) **Labeled Missing sources ( $\mathcal{LM}_r : r = 1, \dots, R$ )** with labeled outcomes but parts of covariates are missing in blocks. In data source  $\mathcal{LM}_r$ , only  $(Y, \mathbf{X}_{\Gamma_r})$  are observed, where  $\Gamma_r \subset \{1, 2, \dots, p\}$  is the index set of the observed covariates, and  $\mathbf{X}_{\mathcal{B}}$  denotes the subvector of  $\mathbf{X}$  containing  $X_j$  for  $j \in \mathcal{B}$ . Let  $\Gamma_r^c = 1, 2, \dots, p \setminus \Gamma_r$  be the complement of  $\Gamma_r$ . For example, if we observe the first two covariates  $(X_1, X_2)$  and  $p = 5$ , then  $\Gamma_r = 1, 2$ ,  $\Gamma_r^c = 3, 4, 5$ ,  $\mathbf{X}_{\Gamma_r} = (X_1, X_2)^\top$ , and  $\mathbf{X}_{\Gamma_r^c} = (X_3, X_4, X_5)^\top$ ; (iii) **Unlabeled Complete ( $\mathcal{UC}$ )** data with unobserved outcomes but fully observed covariates.

This complicated data structure is encountered frequently in real world. For example,  $\mathcal{LC}$  and  $\mathcal{LM}_r$ 's are collected from multiple biomedical studies with the outcome  $Y$  costly to obtain in some larger observational cohort  $\mathcal{UC}$ , as well as covariate structural heterogeneity due to the varying data collection protocols of the studies. Importantly, distributional shifts of covariates across sources are almost inevitable due to the varying measurement standards or patient recruitment criteria. Under such heterogeneity, the usual Missing Completely at Random (MCAR) assumption, which is commonly used in BM data literature, becomes unrealistic as missingness often depends on shared or study-specific covariates. To address this, we incorporate possible distributional shifts across data sources and allow missingness to depend on observed variables, consequently relaxing MCAR to a more flexible Missing At Random (MAR) assumption. This enables more realistic and generalizable data fusion while requiring careful handling of distributional shifts.

Let  $p_{\mathcal{LC}}$ ,  $p_{\mathcal{LM}_r}$  and  $p_{\mathcal{UC}}$  denote the underlying probability density functions for the corresponding data sources. We consider the scenario with distributional shifts across the data sources. In specific, the target population  $\mathcal{UC}$  can have different covariate distribution as  $\mathcal{LC}$  and  $\mathcal{LM}_r$ , i.e.,  $p_{\mathcal{UC}}(\mathbf{X}) \neq p_{\mathcal{LC}, \mathcal{LM}_r}(\mathbf{X})$ , while we assume there exist some *sufficient alignment* sets  $\Omega_0, \Omega_1, \dots, \Omega_R$  of the covariates such that

$$p_{\mathcal{UC}}(Y, \mathbf{X}_{\Omega_0^c} \mid \mathbf{X}_{\Omega_0}) = p_{\mathcal{LC}}(Y, \mathbf{X}_{\Omega_0^c} \mid \mathbf{X}_{\Omega_0}), \quad p_{\mathcal{UC}}(Y, \mathbf{X}_{\Omega_r^c} \mid \mathbf{X}_{\Omega_r}) = p_{\mathcal{LM}_r}(Y, \mathbf{X}_{\Omega_r^c} \mid \mathbf{X}_{\Omega_r}), \quad (1)$$

i.e., the data distributions conditional on  $\mathbf{X}_{\Omega_r}$ 's are aligned and transferable between the labeled and unlabeled samples. When  $\Omega_0 = \{1, \dots, p\}$ , the assumption for  $\mathcal{LC}$  in (1) becomes the conventional covariate shift setting (e.g., Gretton et al., 2009; Liu et al.,

2023). Here, we consider a more general setup to accommodate features  $\mathbf{X}_{\Omega_r^c}$  occurring after  $\mathbf{X}_{\Omega_r}$  (or even  $Y$ ) that are independent of the sampling or enrollment mechanism in  $\mathcal{LM}_r$  given  $\mathbf{X}_{\Omega_r}$ . For BM covariates, we assume that

$$\Omega_r \subseteq \Gamma_r, \quad \forall r \in \{1, 2, \dots, R\} \quad (2)$$

i.e., the sufficient alignment covariates are all observed in  $\mathcal{LM}_r$ . Consequently, we have  $P_{\mathcal{LM}_r}(\mathbf{X}_{\Gamma_r^c} | \mathbf{X}_{\Gamma_r}) = P_{\mathcal{UC}}(\mathbf{X}_{\Gamma_r^c} | \mathbf{X}_{\Gamma_r})$ . In other words, given observed  $\mathbf{X}_{\Gamma_r}$ , the missingness of  $\mathbf{X}_{\Gamma_r^c}$  is independent from its underlying value, i.e.,  $\mathbf{X}_{\Gamma_r^c}$  being MAR. When  $\Omega_r = \emptyset$  for all  $r \in \{0, 1, \dots, R\}$ , (1) is simplified as the MCAR scenario.

We denote  $n$ ,  $n_r$  and  $N$  as the sample sizes of  $\mathcal{LC}$ ,  $\mathcal{LM}_r$  and  $\mathcal{UC}$ , respectively. In the semi-supervised (SS) setting, we assume that  $N \gg n + \sum_{r=1}^R n_r$ . We also define  $\rho_r = n_r/n$ . Our primary goal is to infer a generalized linear model (GLM) on the  $\mathcal{UC}$  population, with the parameter of interest  $\bar{\gamma}$  defined as the solution to the population-level equation:

$$\mathbf{U}(\gamma) = E_{\mathcal{UC}} [\mathbf{A} \{Y - g(\gamma^\top \mathbf{A})\}] = \mathbf{0}, \quad (3)$$

where  $g(\cdot)$  is a known link function with derivative  $\dot{g}$  and  $\mathbf{A}$  is a subset of the covariates in  $\mathbf{X}$  of our interest in terms of risk prediction. For example,  $g(a) = a$  corresponds to a Gaussian linear model, and  $g(a) = e^a/(1 + e^a)$  for the logistic model. When the GLM is correctly specified, i.e.,  $E_{\mathcal{UC}}[Y | \mathbf{A}] = g(\gamma^{*\top} \mathbf{A})$  for some  $\gamma^*$ ,  $\bar{\gamma}$  is identical to the true model parameter  $\gamma^*$ . When the target model is misspecified,  $\bar{\gamma}$  can be viewed as a pseudo-true value that solves the equation (3) and is still useful in practice, e.g., the clinical risk score or polygenic risk score for certain disease (e.g., Elliott et al., 2020). Our method and theory hold regardless of whether this model is correctly specified or not.

In this paper, our primary goal is to leverage and fuse multiple data sources for robust and efficient inference of  $\bar{\gamma}$  defined on the source  $\mathcal{UC}$ . The MAR assumption formalized in (1) enables valid knowledge transfer from data sources that are conditionally aligned on the sufficient alignment sets  $\Omega_r$ . However, in practice, certain BM data sources might violate this assumption, with their distributions of  $(Y, \mathbf{X}_{\Omega_r^c}) | \mathbf{X}_{\Omega_r}$  remain different from the target  $\mathcal{UC}$  population. We refer to such sources as *misaligned*, as they fail to satisfy the MAR condition required for valid fusion. Therefore, identifying and excluding misaligned sources

becomes necessary to preserve the validity of our MAR-based inference. This consideration naturally motivates the development of a screening procedure to detect and remove such bias-prone sources before fusion in Section 2.4.

**Remark 1.** *We allow the inclusion of auxiliary or surrogate features in possibly high-dimensional  $\mathbf{X}_{\Omega_r}$  or  $\mathbf{X}_{\Gamma_r}$  that are informative about  $Y$  or missing covariates but not necessarily included in the target model predictors  $\mathbf{A}$ . This is particularly relevant in EMR applications where a wealth of auxiliary information is routinely collected. For example, in building a risk prediction model for heart disease, the target covariates  $\mathbf{A}$  might include biomarkers that are clinically interpretable and relevant to the disease mechanism. Meanwhile,  $\mathbf{X}$  could contain auxiliary features such as medication codes and clinical mentions strongly correlated with the missing covariates and outcome; see Section 5.2. These auxiliary variables can help aligning the data distributions across the sources or improve the imputation of missing data and enhance estimation efficiency, even though they are excluded from the final scientific model. This distinction between the target predictors  $\mathbf{A}$  and the full  $\mathbf{X}$  allows practitioners to maintain interpretability in the target model while leveraging the predictive power of high-dimensional or AI-generated auxiliary features (e.g., Angelopoulos et al., 2023a).*

### 1.3 Related Literature

As more data is combined from different institutions, blockwise missing covariates have become an important problem. Several recent works have been designed for BM data to achieve more robust and efficient estimation. Yu et al. (2020) proposed an approach for integrative linear regression under BM. Xue and Qu (2021) proposed to aggregate linear estimating equations with multi-source imputed data sets to achieve an efficiency gain. Xue et al. (2021) further extended this framework for high-dimensional inference. Song et al. (2024) applied the idea of debiasing to handle BM without imputations, and Jin and Rothenhäusler (2023) proposed a modular regression approach for multi-modal covariates. These models focused on the linear model only. For GLM allowing nonlinear links, (Li et al., 2023) proposed a penalized estimating equation approach with multiple imputation. Zhao et al. (2023) introduced a generalized method of moments (GMM) approach to incorporate

the BM data. Their methods fit a GLM to the BM data using available covariates only and then using this “reduced” working model to improve the estimation of the target model. Similar strategies were also used in Song et al. (2024) and others with different formulations. For example, Wang et al. (2023) derived calibration weights based on the moment condition of the BM’s reduced model, and used them to reweight the complete data to improve estimation efficiency. This idea dates back to the model-calibration method for survey data with auxiliary information (Wu and Sitter, 2001).

The pursuit of semiparametric efficiency has been a central theme in missing data literature. The seminal work of Robins et al. (1994) established the theory of efficient estimation with missing covariates. Recent advances have further addressed the BM problems. For instance, Li and Luedtke (2023) developed the efficient influence function for fusing longitudinal data with BM structures and proposed a canonical gradient method for implementation. Qiu et al. (2024) proposed multiply robust estimators that achieve efficiency under general forms of dataset shift. This track represents the state-of-the-art in terms of theoretical efficiency. However, their practical implementation faces challenges in complex settings. First, their efficiency gains remain sensitive to model misspecification of nuisance models. Second, the construction of efficient estimators for our non-monotonically missing data often requires recursive fitting of many nuisance models, which poses computational difficulties and convergence issues especially when incorporating machine learning.

The two lines of work reviewed above do not explicitly address the practical issue of source misalignment, where distributional differences between data sources may violate the alignment assumptions like (1) required for valid inference. Recent work (e.g., Cheng and Cai, 2021; Han et al., 2025) addressed this problem through sensitivity analyses that leverage the difference of certain summary statistics to examine the alignment between sources and exclude misaligned ones. Yang et al. (2023) and Chen et al. (2025) considered a similar adaptive fusion strategy when combining experimental and observational studies for inference of treatment effects.

Our work also aligns with the recent progress in semi-supervised learning, which leverage large unlabeled datasets to enhance statistical efficiency when labeled data are limited. For example, (Kawakita and Kanamori, 2013) and (Song et al., 2023) proposed to reweight the regression on the labeled sample with estimated density ratios. (Chakraborty and Cai,

2018) and (Gronsbell et al., 2022) imputed its unobserved outcome  $Y$ . (Wu and Liu, 2023) extended this imputation framework for SSL of graphic models. These SSL methods can produce more efficient estimates than their supervised learning (SL) counterpart when the outcome model is misspecified while they remain as efficient as SL when that model is correct. Recently, Liu et al. (2023), Zhang et al. (2023) and others extended SSL to handle covariate shifts through doubly robust estimation, but their framework does not accommodate the complex blockwise missing structures prevalent in fused data sources.

## 1.4 Our contribution

We propose a novel **Data-adaptive Estimation** approach for data **F**usion in the **S**Emi-supervised setting (DEFUSE). It systematically handles both blockwise missingness and semi-supervised problems in the MAR setting through three key methodological innovations. They are supported by asymptotic analysis, simulations, and real-world applications.

First, we introduce a novel data-adaptive calibration approach for fusing BM data under MAR. Unlike existing methods that rely on rigid semiparametric efficient or reduced working model strategies, our framework employs a family of calibrated control functions that maintain valid statistical inference while achieving efficiency gains. Compared to several tracks of existing work reviewed above, our method has three key advantages. **Data-adaptivity:** Our approach is adaptive to arbitrary BM patterns of covariates as well as model misspecification in the control variates, and automatically adjusts to the degree of distributional shifts. **Intrinsic efficiency:** Our method achieves optimal performance within user-specified classes of calibration functions broader than those in existing work. **Computational feasibility and flexibility:** The control variates can be constructed based on generic ML and the calibration procedure is computationally tractable through finite-dimensional quadratic programming, accommodating both parametric and kernel ridge regression. These grant us a better tradeoff between computational costs and statistical efficiency, being more practical than pursuing semiparametric efficiency via recursive fitting of nuisance models, particularly with high-dimensional auxiliary features.

Second, we develop a novel screening procedure to **identify and exclude misaligned data sources**. Recognizing that certain distributional shifts can violate the MAR assump-

tion in practical settings, we develop a debiased discrepancy measure method based on the mean squared difference of certain conditional mean model between sources. This screening mechanism prioritizes statistical validity by automatically detecting and excluding BM sources not sufficiently aligned with the target  $\mathcal{UC}$  population. Compared to most existing fusion methods that assume perfect transportability, our approach provides protection against bias from misaligned sources while maintaining power to detect truly transportable ones. Also, our approach is rigorously sharper than the commonly used sensitivity analysis strategy based on the mean difference of certain statistics between sources.

Third, we introduce a **semi-supervised framework** that leverages large unlabeled samples to further enhance efficiency of the BM-fused estimator. By projecting the estimator onto the function space of fully observed covariates, we achieve strictly smaller asymptotic variance than the estimator using only  $\mathcal{LC}$  and  $\mathcal{LM}_r$  samples. This advancement reflects a more effective utilization of the  $\mathcal{UC}$  samples in BM fusion problems compared to existing approaches. Collectively, these innovations enable DEFUSE to achieve robust and efficient data fusion under realistic conditions where blockwise missingness, semi-supervised learning, and distributional shifts coexist.

## 2 Method

### 2.1 Preliminary Estimation

Consider the problem of inferring a linear functional of  $\boldsymbol{\gamma}$ , denoted by  $\mathbf{c}^\top \boldsymbol{\gamma}$ , where  $\mathbf{c}$  is an arbitrary vector with  $\|\mathbf{c}\|_2 = 1$ . When the goal is to estimate the full vector  $\boldsymbol{\gamma}$ , we set  $\mathbf{c} = \mathbf{e}_j$ , the  $j$ -th unit vector in  $\mathbb{R}^p$ , i.e.,  $\mathbf{c}^\top \boldsymbol{\gamma} = \gamma_j$ . We then apply the following method to estimate each  $\bar{\gamma}_j$  for  $j = 1, \dots, p$ , and combine the resulting scalar estimates to form the final estimator of  $\bar{\boldsymbol{\gamma}}$ . For predictive applications with a new subject of covariate  $\mathbf{A}_{\text{new}} \neq \mathbf{0}$ , one can take  $\mathbf{c} = \mathbf{A}_{\text{new}} / \|\mathbf{A}_{\text{new}}\|_2$ , estimate  $\mathbf{c}^\top \boldsymbol{\gamma}$ , and use  $\|\mathbf{A}_{\text{new}}\|_2 \mathbf{c}^\top \boldsymbol{\gamma}$  as the linear predictor. Let  $\widehat{\mathbb{E}}_{\mathcal{D}}[f(\cdot)]$  denote the empirical mean of a measurable function  $f(d)$  over observations  $d \in \mathcal{D}$ , where  $\mathcal{D}$  is a subset of  $\{\mathcal{LC}, \mathcal{LM}_r, \mathcal{UC}\}$ , e.g.,  $\widehat{\mathbb{E}}_{\mathcal{LC}}[f] = \frac{1}{n} \sum_{d \in \mathcal{LC}} f(d)$ . Similarly, we define  $\widehat{\text{Var}}_{\mathcal{D}}[f]$  as the empirical variance of  $f(\cdot)$  on the dataset  $\mathcal{D}$ , e.g.,  $\widehat{\text{Var}}_{\mathcal{LC}}[f] = \frac{1}{n} \sum_{d \in \mathcal{LC}} \left\{ f(d) - \widehat{\mathbb{E}}_{\mathcal{LC}}[f] \right\}^2$ . Let  $r_{\mathcal{LC}}(\mathbf{X}_{\Omega_0}) = p_{\mathcal{UC}}(\mathbf{X}_{\Omega_0}) / p_{\mathcal{LC}}(\mathbf{X}_{\Omega_0})$  and  $r_{\mathcal{LM}_r}(\mathbf{X}_{\Omega_r}) = p_{\mathcal{UC}}(\mathbf{X}_{\Omega_r}) / p_{\mathcal{LM}_r}(\mathbf{X}_{\Omega_r})$  be the true

density ratio function of the sufficient alignment covariates between  $\mathcal{UC}$  and  $\mathcal{LC}/\mathcal{LM}_r$ . For two sequences  $a_n$  and  $b_n$ , we denote by  $a_n = O(b_n)$  if  $\lim_{n \rightarrow \infty} |a_n/b_n| < \infty$ ,  $a_n = o(b_n)$  if  $\lim_{n \rightarrow \infty} a_n/b_n = 0$ , and  $a_n = o_{\mathbb{P}}(b_n)$  or  $a_n = O_{\mathbb{P}}(b_n)$  if  $a_n = o(b_n)$  or  $a_n = O(b_n)$  with a probability approaching 1.

First, we derive a preliminary estimator for  $\bar{\gamma}$  using the  $\mathcal{LC}$  and  $\mathcal{UC}$  samples. Due to the distributional shift of  $\mathbf{X}_{\Omega_0}$  between  $\mathcal{LC}$  and  $\mathcal{UC}$ , directly solving the standard estimating equation in (3) with  $\mathcal{LC}$  will lead to bias. The conventional importance weighting method (Gretton et al., 2009) adjusts for this bias by reweighting  $\mathcal{LC}$  samples with the density ratio  $r_{\mathcal{LC}}(\mathbf{X}_{\Omega_0})$  and can produce a consistent estimator for  $\bar{\gamma}$  under assumption (1). However, due to the excessive error of machine learning (ML) estimation for  $r_{\mathcal{LC}}(\cdot)$ , this strategy tends to fail in achieving  $n^{1/2}$ -consistency or asymptotic unbiasedness (Liu et al., 2023). To address this issue, we introduce the double/debiased machine learning (DML) operators:

$$\begin{aligned}\mathfrak{M}_{\mathcal{LC}}(D) &= r_{\mathcal{LC}}(\mathbf{X}_{\Omega_0})(D - E_{\mathcal{LC}}[D | \mathbf{X}_{\Omega_0}]) + E_{UC}(E_{\mathcal{LC}}[D | \mathbf{X}_{\Omega_0}]), \\ \mathfrak{M}_{\mathcal{LM}_r}(D) &= r_{\mathcal{LM}_r}(\mathbf{X}_{\Omega_r})(D - E_{\mathcal{LM}_r}[D | \mathbf{X}_{\Omega_r}]) + E_{UC}(E_{\mathcal{LM}_r}[D | \mathbf{X}_{\Omega_r}]),\end{aligned}\tag{4}$$

where  $D$  can be any function of variables observed in  $\mathcal{LC}$  or  $\mathcal{LM}_r$ . Let  $\hat{r}_{\mathcal{LC}}(\mathbf{Z})$ ,  $\hat{r}_{\mathcal{LM}}(\mathbf{Z})$ ,  $\hat{E}_{\mathcal{LC}}[D | \mathbf{X}_{\Omega_0}]$  and  $\hat{E}_{\mathcal{LM}_r}[D | \mathbf{X}_{\Omega_r}]$  denote ML estimators of the nuisance functions  $r_{\mathcal{LC}}(\mathbf{X}_{\Omega_0})$ ,  $r_{\mathcal{LM}}(\mathbf{X}_{\Omega_r})$ ,  $E_{\mathcal{LC}}[D | \mathbf{X}_{\Omega_0}]$  and  $E_{\mathcal{LM}_r}[D | \mathbf{X}_{\Omega_r}]$ , respectively. We use  $\widehat{\mathfrak{M}}_{\mathcal{LC}}(\cdot)$  to represent the empirical version of  $\mathfrak{M}_{\mathcal{LC}}(\cdot)$ , with  $r_{\mathcal{LC}}$ ,  $E_{\mathcal{LC}}[\cdot | \mathbf{X}_{\Omega_0}]$ , and  $E_{UC}$  in (4) replaced by their estimators or empirical counterpart  $\hat{r}_{\mathcal{LC}}$ ,  $\hat{E}_{\mathcal{LC}}[\cdot | \mathbf{X}_{\Omega_0}]$ , and  $\hat{E}_{UC}$ , and define  $\mathfrak{M}_{\mathcal{LM}_r}(\cdot)$  in the same way. In the MCAR scenario with  $\Omega_r = \emptyset$  for  $r = 0, \dots, R$ , we trivially have  $\widehat{\mathfrak{M}}_{\mathcal{LC}}(D) = \widehat{\mathfrak{M}}_{\mathcal{LM}}(D) = D$ . Then, we obtain the preliminary estimator  $\tilde{\gamma}$  by solving

$$\tilde{\mathbf{U}}_{\mathcal{LC}}(\gamma) = \hat{E}_{\mathcal{LC}} \left[ \widehat{\mathfrak{M}}_{\mathcal{LC}}(\mathbf{A}\{Y - g(\gamma^\top \mathbf{A})\}) \right] = \mathbf{0}.\tag{5}$$

The asymptotic expansion of  $\tilde{\gamma}$  is established in Lemma 1 under the regularity and ML convergence assumptions presented in Appendix. We require the ML estimators of the density ratio and conditional mean models converge to the truth in the rate  $o_{\mathbb{P}}(n^{-1/4})$ .

**Lemma 1.** *Under Assumptions A1 - A2, we have*

$$\sqrt{n}(\tilde{\gamma} - \bar{\gamma}) = \sqrt{n}\hat{E}_{\mathcal{LC}}\mathfrak{M}_{\mathcal{LC}}(\bar{\mathbf{S}}) + o_{\mathbb{P}}(1),$$

where  $\bar{\mathbf{S}} \equiv \bar{\mathbf{S}}(\mathbf{A}, Y) = \bar{\mathbf{J}}^{-1} \mathbf{A} \{Y - g(\bar{\boldsymbol{\gamma}}^\top \mathbf{A})\}$  and  $\bar{\mathbf{J}} = \text{E}_{uc}[\dot{g}(\bar{\boldsymbol{\gamma}}^\top \mathbf{A}) \mathbf{A} \mathbf{A}^\top]$ . Also,  $\sqrt{n}(\tilde{\boldsymbol{\gamma}} - \bar{\boldsymbol{\gamma}})$  weakly converge to gaussian distribution with mean zero.

The preliminary estimation introduced above can be implemented with generic ML methods (e.g., random forests or neural networks) for estimating the nuisance functions. To ensure the asymptotic validity, we employ cross-fitting as used in Chernozhukov et al. (2016), which avoids overfitting and guarantees asymptotic unbiasedness. To further reduce computational costs, we propose an implementation procedure initializing with the importance weighting estimator using  $\hat{r}_{\mathcal{L}\mathcal{C}}(\cdot)$ , followed by an one-step Newton-Raphson update based on (5). This one-step estimator can be shown to be asymptotically equivalent to the fully iterative solution of (5), while being computationally more economical. Details of the cross-fitting and one-step estimation are presented in Appendix. For notational simplicity, we drop the subscripts indicating the split data folds in our main paper.

## 2.2 Control Variate and Data-adaptive Calibration

After obtaining the preliminary  $\tilde{\boldsymbol{\gamma}}$ , we incorporate the  $\mathcal{L}\mathcal{M}_r$  samples to reduce its variance. For now, assume the alignment assumption depicted by (1) and (2) holds for all sources. The scenario with misaligned sources will be considered in Section 2.4. By Lemma 1, the asymptotic variance of  $\mathbf{c}^\top \tilde{\boldsymbol{\gamma}}$  is proportional to that of  $\mathbf{c}^\top \mathfrak{M}_{\mathcal{L}\mathcal{C}}(\bar{\mathbf{S}})$ . Inspired by the control variate approach (Glasserman, 2004), our first idea is to augment  $\mathbf{c}^\top \tilde{\boldsymbol{\gamma}}$  as:

$$\beta^\dagger = \mathbf{c}^\top \tilde{\boldsymbol{\gamma}} + \sum_{r=1}^R \left\{ \hat{\text{E}}_{\mathcal{L}\mathcal{M}_r} \left[ \widehat{\mathfrak{M}}_{\mathcal{L}\mathcal{M}_r}(\tilde{\phi}_{1,r}) \right] - \hat{\text{E}}_{\mathcal{L}\mathcal{C}} \left[ \widehat{\mathfrak{M}}_{\mathcal{L}\mathcal{C}}(\tilde{\phi}_{1,r}) \right] \right\}, \quad (6)$$

where  $\tilde{\phi}_{1,r} \equiv \tilde{\phi}_{1,r}(\mathbf{X}_{\Gamma_r}, Y)$  is some data-dependent control function of the observed variables in  $\mathcal{L}\mathcal{M}_r$ . Again, we use the DML operators  $\widehat{\mathfrak{M}}_{\mathcal{L}\mathcal{C}}$  and  $\widehat{\mathfrak{M}}_{\mathcal{L}\mathcal{M}_r}$  on the control functions to correct bias due to distributional shifts. We can show that under the MAR assumption (1) and the regularity and rate assumptions introduced in Section 3, the augmentation terms such as  $\hat{\text{E}}_{\mathcal{L}\mathcal{M}_r}[\widehat{\mathfrak{M}}_{\mathcal{L}\mathcal{M}_r}(\tilde{\phi}_{1,r})] - \hat{\text{E}}_{\mathcal{L}\mathcal{C}}[\widehat{\mathfrak{M}}_{\mathcal{L}\mathcal{C}}(\tilde{\phi}_{1,r})]$  are asymptotically mean-zero and only affect the variance of  $\beta^\dagger$ . Consequently,  $\beta^\dagger$  is still valid, while its variance could be potentially smaller than the preliminary estimator  $\mathbf{c}^\top \tilde{\boldsymbol{\gamma}}$  when  $\tilde{\phi}_{1,r}$  is specified properly.

We specify the control variate as an estimator of  $\phi_{1,r}^*(\mathbf{X}_{\Gamma_r}, Y) := \frac{\rho_r}{1+\rho_r} \text{E}_{\mathcal{L}\mathcal{C}}[\mathbf{c}^\top \bar{\mathbf{S}} | \mathbf{X}_{\Gamma_r}, Y]$ ,

which offers a moderately advantageous alternative compared to existing work; see our simulation results in Section 4. Empirically, let  $\tilde{\mathbf{S}} \equiv \tilde{\mathbf{S}}(\mathbf{A}, Y)$  be an estimate of  $\bar{\mathbf{S}}(\mathbf{A}, Y)$  with  $\bar{\boldsymbol{\gamma}}$  replaced by the preliminary  $\tilde{\boldsymbol{\gamma}}$ . We obtain  $\tilde{\phi}_{1,r}$  by estimating  $\phi^*$  using the  $\mathcal{LC}$  sample, either by (1) directly regressing  $\mathbf{c}^\top \tilde{\mathbf{S}}$  against  $\{\mathbf{X}_{\Gamma_r}, Y\}$ , or (2) learning the conditional distribution  $\mathbf{X}_{\Gamma_r^c} | \mathbf{X}_{\Gamma_r}, Y$  and computing the conditional mean of  $\mathbf{c}^\top \tilde{\mathbf{S}}$  via Monte Carlo methods. Crucially, the unbiasedness of  $\beta^\dagger$  is preserved even if  $\tilde{\phi}_{1,r}$  does not converge to  $\phi^*$ . We emphasize that while we focus on the specific  $\phi_r^*(\mathbf{X}_{\Gamma_r}, Y)$  here, our calibration method introduced below can naturally accommodate other choices of the control function. This flexibility allows practitioners to tailor the control function to specific contexts while still benefiting from our framework.

Let  $\mathbf{Z}_r \subseteq \{\mathbf{X}_{\Gamma_r}, Y\}$  be some prespecified vector of variables. The key idea is to calibrate  $\tilde{\phi}_{1,r}$  through a reweighting function  $w_r(\mathbf{Z}_r; \boldsymbol{\delta}_r)$ , which leads to the calibrated estimator:

$$\hat{\beta}_1(\boldsymbol{\delta}) = \mathbf{c}^\top \tilde{\boldsymbol{\gamma}} + \sum_{r=1}^R \left\{ \hat{\mathbb{E}}_{\mathcal{LM}_r} \left[ \widehat{\mathfrak{M}}_{\mathcal{LM}_r}(\tilde{\varphi}_{1,r}(\boldsymbol{\delta}_r)) \right] - \hat{\mathbb{E}}_{\mathcal{LC}} \left[ \widehat{\mathfrak{M}}_{\mathcal{LC}}(\tilde{\varphi}_{1,r}(\boldsymbol{\delta}_r)) \right] \right\}, \quad (7)$$

where  $\tilde{\varphi}_{1,r}(\boldsymbol{\delta}_r) \equiv \tilde{\varphi}_{1,r}(\mathbf{X}_{\Gamma_r}, Y, \boldsymbol{\delta}_r) = \tilde{\phi}_{1,r}(\mathbf{X}_{\Gamma_r}, Y) w_r(\mathbf{Z}_r; \boldsymbol{\delta}_r)$  is an augmented control variate, and  $\boldsymbol{\delta} = \{\boldsymbol{\delta}_r : r = 1, \dots, R\}$  encodes calibration parameters of the prespecified model  $w_r(\cdot; \boldsymbol{\delta}_r)$ . Among the parameter space of  $\boldsymbol{\delta}$  denoted as  $\mathcal{C}_\delta$ , the optimal  $\boldsymbol{\delta}$  should minimize the asymptotic variance of  $\hat{\beta}_1(\boldsymbol{\delta})$ , which can be viewed as *intrinsic efficiency* (e.g., Tan, 2010; Rotnitzky et al., 2012). Thus, we propose to solve  $\tilde{\boldsymbol{\delta}} = \{\tilde{\boldsymbol{\delta}}_r : r = 1, \dots, R\}$  from quadratic programming:

$$\tilde{\boldsymbol{\delta}} = \arg \min_{\boldsymbol{\delta} \in \mathcal{C}_\delta} \widehat{Q}(\boldsymbol{\delta}), \quad (8)$$

where  $\widehat{Q}(\boldsymbol{\delta})$  is the empirical variance of  $n^{1/2}(\hat{\beta}_1(\boldsymbol{\delta}) - \mathbf{c}^\top \tilde{\boldsymbol{\gamma}})$  defined as:

$$\widehat{Q}(\boldsymbol{\delta}) = \widehat{\text{Var}}_{\mathcal{LC}} \left[ \widehat{\mathfrak{M}}_{\mathcal{LC}} \left( \mathbf{c}^\top \tilde{\mathbf{S}} - \sum_{r=1}^R \tilde{\varphi}_{1,r}(\boldsymbol{\delta}_r) \right) \right] + \sum_{r=1}^R \frac{1}{\rho_r} \widehat{\text{Var}}_{\mathcal{LM}_r} \left[ \widehat{\mathfrak{M}}_{\mathcal{LM}_r}(\tilde{\varphi}_{1,r}(\boldsymbol{\delta}_r)) \right].$$

Then we obtain the data-adaptive estimator  $\hat{\beta}_1 \equiv \hat{\beta}_1(\boldsymbol{\delta})$  that is also denoted as  $\text{DEFUSE}_{\mathcal{LM}}$ .

Unlike typical regression tasks targeting conditional mean models, (8) may not be computationally feasible or, at least, sophisticated to solve in practice when the weight  $w_r(\cdot)$  is taken as a generic ML model. This is due to the presence of the DML operators  $\widehat{\mathfrak{M}}_{\mathcal{LC}}$  and

$\widehat{\mathfrak{M}}_{\mathcal{LM}_r}$  as well as the addition of multiple  $\tilde{\varphi}_{1,r}(\boldsymbol{\delta}_r)$ 's supported on different sets of variables in (8). To address this concern, we recommend in Examples 1–3 specific choices for  $w_r(\cdot)$ , covering both parametric and nonparametric models. Notably, all of them can be directly computed via finite-dimensional quadratic programming. Example 1 simply uses constant calibration coefficients to re-allocate the data sources  $\mathcal{LM}_r$ 's, which has a similar spirit as some recent advances in PPI and SSL (e.g., Angelopoulos et al., 2023b; Miao et al., 2023). Compared to this, Examples 2 and 3 enable more powerful calibration as demonstrated in Section 4. Example 2 specifies  $w_r(\mathbf{Z}_r)$  as a linear function and Example 3 realizes computationally tractable nonparametric calibration via kernel ridge regression (KRR).

**Example 1** (Simple allocation). *Set  $w_r(\mathbf{Z}_r) = \delta_r$  with  $\delta_r \in \mathbb{R}$ .*

**Example 2** (Linear function). *Set  $w_r(\mathbf{Z}_r) = (1, \mathbf{Z}_r^\top)\boldsymbol{\delta}_r$  with  $\boldsymbol{\delta}_r \in \mathbb{R}^{\dim(\mathbf{Z}_r)+1}$ .*

**Example 3** (Kernel ridge regression). *Set  $w_r(\mathbf{Z}_r)$  to be from a reproducing kernel Hilbert space (RKHS) induced by a symmetric and positive semi-definite kernel  $K_r(\cdot, \cdot)$  on the domain of  $\mathbf{Z}_r$ . By Moore–Aronszajn Theorem (Aronszajn, 1950), there exist some Hilbert space  $\mathcal{H}$  and feature map  $\xi$  such that  $\langle \xi(\mathbf{u}), \xi(\mathbf{v}) \rangle_{\mathcal{H}} = K_r(\mathbf{u}, \mathbf{v})$  where  $\langle \cdot, \cdot \rangle_{\mathcal{H}}$  is the inner product on  $\mathcal{H}$ . Then, we can write  $w_r(\cdot) \in \mathcal{W}_r := \{ \langle \xi(\cdot), \boldsymbol{\theta}_r \rangle_{\mathcal{H}} : \boldsymbol{\theta}_r \in \mathcal{H} \}$  and its finite-sample approximation  $w_r(\mathbf{z}; \boldsymbol{\delta}_r) = n^{-1} \sum_{i=1}^n \delta_{r,i} K_r(\mathbf{z}, \mathbf{Z}_{r,i})$ , where  $\mathbf{Z}_{r,i}$  represents the  $i$ -th observation of  $\mathbf{Z}_r$  in  $\mathcal{LC}$ . Based on this, we can solve for the calibration parameters  $\boldsymbol{\delta}_r$ 's through finite-dimensional quadratic programming:  $\tilde{\boldsymbol{\delta}} = \arg \min_{\boldsymbol{\delta}} \widehat{Q}(\boldsymbol{\delta}) + \sum_{r=1}^R \lambda_r \|\boldsymbol{\delta}_r\|_2^2$ , where  $\lambda_r$  is a regularization parameter.*

## 2.3 Semi-supervised Estimation

For the  $\mathcal{LC}$ -based terms composing  $\widehat{\beta}_1(\boldsymbol{\delta})$  in (7), an interesting observation is that the asymptotic expansion of  $\mathbf{c}^\top \tilde{\boldsymbol{\gamma}}$ , i.e., term  $\mathbf{c}^\top \mathfrak{M}_{\mathcal{LC}}(\bar{\mathbf{S}})$  is strictly or nearly orthogonal to  $\mathbf{X}$  when  $\mathbf{A} = \mathbf{X}$  and the target GLM is correctly specified or not severely misspecified. This poses a fundamental limit to the efficiency gains achievable by existing SSL methods in the standard SS setting with  $\mathcal{LC}$  and  $\mathcal{UC}$  only (e.g., Chakraborty and Cai, 2018), because their estimators are derived by projecting the expansion of  $\mathbf{c}^\top \tilde{\boldsymbol{\gamma}}$  onto the function space of  $\mathbf{X}$ . In contrast, our introduced  $\tilde{\varphi}_{1,r}(\mathbf{X}_{\Gamma_r}, Y; \tilde{\boldsymbol{\delta}})$  only depends on the subset  $\Gamma_r$  of  $\mathbf{X}$  and, thus, is typically *not* orthogonal to  $\mathbf{X}$ . Consequently, the  $\mathcal{LC}$ -components in

(7) satisfies that  $E_{\mathcal{L}\mathcal{C}}[\bar{S}_1 | \mathbf{X}] \neq 0$ , where  $\bar{S}_1 \equiv \bar{S}_1(\mathbf{X}, Y)$  is the population version of  $\tilde{S}_1(\mathbf{X}, Y) := \mathbf{c}^\top \tilde{\mathbf{S}}(\mathbf{A}, Y) - \sum_{r=1}^R \tilde{\varphi}_{1,r}(\mathbf{X}_{\Gamma_r}, Y; \tilde{\boldsymbol{\delta}}_r)$ .

This phenomenon motivates us to further incorporate the  $\mathcal{UC}$  sample to reduce the variance of the  $\text{DEFUSE}_{\mathcal{L}\mathcal{M}}$  estimator. Similarly, this step involves control variates with data-adaptive calibration. In specific, we introduce  $\tilde{\phi}_2(\mathbf{X})$  as an estimate of  $E_{\mathcal{L}\mathcal{C}}[\bar{S}_1 | \mathbf{X}]$  and its calibrated version as  $\tilde{\varphi}_2(\boldsymbol{\zeta}) \equiv \tilde{\varphi}_2(\mathbf{X}; \boldsymbol{\zeta}) = \tilde{\phi}_2(\mathbf{X})h(\mathbf{X}; \boldsymbol{\zeta})$  where  $h$  is a reweighting function parameterized by  $\boldsymbol{\zeta} \in \mathcal{C}_\zeta$ . The estimator is then formed as:

$$\hat{\beta}_2(\boldsymbol{\zeta}) = \hat{\beta}_1 + \hat{E}_{\mathcal{UC}}[\tilde{\varphi}_2(\boldsymbol{\zeta})] - \hat{E}_{\mathcal{L}\mathcal{C}}[\widehat{\mathfrak{M}}_{\mathcal{L}\mathcal{C}}(\tilde{\varphi}_2(\boldsymbol{\zeta}))], \quad (9)$$

and the optimal calibration parameter is solved from

$$\tilde{\boldsymbol{\zeta}} = \arg \min_{\boldsymbol{\zeta} \in \mathcal{C}_\zeta} \hat{T}(\boldsymbol{\zeta}), \quad \text{where} \quad \hat{T}(\boldsymbol{\zeta}) = \widehat{\text{Var}}_{\mathcal{L}\mathcal{C}} \left[ \widehat{\mathfrak{M}}_{\mathcal{L}\mathcal{C}}(\tilde{S}_1(\mathbf{X}, Y) - \tilde{\varphi}_2(\boldsymbol{\zeta})) \right] + \text{const}. \quad (10)$$

The final  $\text{DEFUSE}$  estimator is then constructed as  $\hat{\beta}_2 \equiv \hat{\beta}_2(\tilde{\boldsymbol{\zeta}})$ . The calibration function  $h(\cdot)$  could be specified using the same strategies as Examples 1–3. Compared to  $\hat{Q}(\boldsymbol{\delta}_1, \dots, \boldsymbol{\delta}_R)$  used in (8),  $\hat{T}(\boldsymbol{\zeta})$  in (10) does not include the variance term of  $\tilde{\varphi}_2$ . This is because the contributed variance of  $\tilde{\varphi}_2$  over  $\mathcal{UC}$  is negligible in the SS setting with  $N \gg n$ .

## 2.4 Exclude Misaligned Data Sources

Prior to integrating the BM data sources, it is crucial to assess their transferability to the target population  $\mathcal{UC}$ , i.e., whether the MAR assumption in (1) holds. In many practical applications, the  $\mathcal{LC}$  sample can usually serve as a reliable benchmark for this purpose, e.g., when the  $\mathcal{LC}$  and  $\mathcal{UC}$  samples are concurrently collected under a unified protocol, featuring fully-observed covariates  $\mathbf{X}$ . In contrast, the  $\mathcal{LM}_r$  sources may originate from historical studies, external databases, or different institutions where specific features were not collected or defined consistently, leading to the BM pattern. In such settings, it is reasonable to posit that  $\mathcal{LC}$  and  $\mathcal{UC}$  are well-aligned, i.e., the first equation of (1) holds. Suppose this holds, and consequently, we can leverage  $\mathcal{LC}$  as a reference to identify sources  $\mathcal{LM}_r$ 's that exhibit significant deviation from the MAR assumption and thus should be excluded from data fusion to avoid bias.

For simplicity, we assume  $\Omega_0 \subseteq \Omega_r$  for now. Our proposal for the generic setup without this will be introduced later. Recall (7) that the influence from  $\mathcal{LM}_r$  is characterized by the control variate  $\tilde{V}_r \equiv \widehat{\text{E}}_{\mathcal{LM}_r} [\widehat{\mathfrak{M}}_{\mathcal{LM}_r}(\tilde{\varphi}_{1,r}(\tilde{\boldsymbol{\delta}}_r))] - \widehat{\text{E}}_{\mathcal{LC}} [\widehat{\mathfrak{M}}_{\mathcal{LC}}(\tilde{\varphi}_{1,r}(\tilde{\boldsymbol{\delta}}_r))]$ . One can show that  $\tilde{V}_r$  converges to  $\bar{V}_r \equiv \text{E}_{\mathcal{UC}} [m_r(\mathbf{X}_{\Omega_r}) - m_r^*(\mathbf{X}_{\Omega_r})]$ , where  $m_r(\mathbf{X}_{\Omega_r}) = \text{E}_{\mathcal{LM}_r} [\tilde{\varphi}_{1,r}(\mathbf{X}_{\Gamma_r}, Y, \tilde{\boldsymbol{\delta}}_r) \mid \mathbf{X}_{\Omega_r}, \tilde{\varphi}_{1,r}, \tilde{\boldsymbol{\delta}}_r]$  and  $m_r^*(\mathbf{X}_{\Omega_r}) = \text{E}_{\mathcal{LC}} [\tilde{\varphi}_{1,r}(\mathbf{X}_{\Gamma_r}, Y, \tilde{\boldsymbol{\delta}}_r) \mid \mathbf{X}_{\Omega_r}, \tilde{\varphi}_{1,r}, \tilde{\boldsymbol{\delta}}_r]$ . When (1) fails for  $\mathcal{LM}_r$ , it is likely that  $\bar{V}_r \neq 0$ , which induces bias to our estimator. In this situation, it is wise to exclude  $\mathcal{LM}_r$ . To effectively identify such bias-prone sources, we introduce the mean squared discrepancy (MSD) measure:  $\bar{\Delta}_r^2 = \text{E}_{\mathcal{UC}} [m_r(\mathbf{X}_{\Omega_r}) - m_r^*(\mathbf{X}_{\Omega_r})]^2$ . When the MAR assumption (1) holds for  $\mathcal{LM}_r$  and  $\Omega_0 \subseteq \Omega_r$ ,  $(\mathbf{X}_{\Gamma_r}, Y) \mid \mathbf{X}_{\Omega_r}$  remains to be the same between  $\mathcal{LC}$  and  $\mathcal{LM}_r$ , indicating that  $\bar{\Delta}_r = 0$ ; otherwise,  $\bar{\Delta}_r$  tends to be larger than zero. Thus, we aim to exclude  $\mathcal{LM}_r$  from data fusion if  $r \in \mathcal{A}^c$  where the set of aligned sources  $\mathcal{A} = \{r : \bar{\Delta}_r = 0\}$  and  $\mathcal{A}^c = \{1, \dots, R\} \setminus \mathcal{A}$ . Importantly, since  $|\bar{V}_r| \leq \bar{\Delta}_r$ ,  $\bar{\Delta}_r$  is a sharper and more sensitive measure for the violation of MAR compared to the mean difference  $\bar{V}_r$  commonly used for sensitivity analysis in data fusion (e.g., Cheng and Cai, 2021; Han et al., 2025).

Empirically, suppose we obtain  $\widehat{m}_r(\cdot)$  and  $\widehat{m}_r^*(\cdot)$  as the ML estimators for  $m_r(\cdot)$  and  $m_r^*(\cdot)$ , respectively. Simply plugging in  $\widehat{m}_r(\cdot)$  and  $\widehat{m}_r^*(\cdot)$  to estimate MSD could result in excessive ML bias that dominates the actual  $\bar{\Delta}_r$ . To address this issue, we propose a debiasing method. Suppose  $\mathcal{G}$  is a prespecified function space satisfying (i)  $\text{E}_{\mathcal{UC}} [h^2(\mathbf{x}_{\Omega_r})] \leq 1$  for all  $h \in \mathcal{G}$  and (ii)  $h^* \in \mathcal{G}$ , where  $h^*(\mathbf{x}_{\Omega_r}) := \{m_r(\mathbf{x}_{\Omega_r}) - m_r^*(\mathbf{x}_{\Omega_r})\} / \{\text{E}_{\mathcal{UC}} [m_r(\mathbf{x}_{\Omega_r}) - m_r^*(\mathbf{x}_{\Omega_r})]^2\}^{1/2}$  if  $m_r(\mathbf{x}_{\Omega_r}) - m_r^*(\mathbf{x}_{\Omega_r}) \neq 0$  and  $h^*(\mathbf{x}_{\Omega_r}) := 1$ , otherwise. Then we have

$$\bar{\Delta}_r = \max_{h \in \mathcal{G}} L(h), \quad \text{where } L(h) = \text{E}_{\mathcal{UC}} [h(\mathbf{X}_{\Omega_r}) \{m_r(\mathbf{X}_{\Omega_r}) - m_r^*(\mathbf{X}_{\Omega_r})\}]. \quad (11)$$

We construct the debiased estimator for the objective function  $L(h)$  as:

$$\begin{aligned} \widehat{L}(h) = & \widehat{\text{E}}_{\mathcal{UC}} [h(\mathbf{X}_{\Omega_r}) \{\widehat{m}_r(\mathbf{X}_{\Omega_r}) - \widehat{m}_r^*(\mathbf{X}_{\Omega_r})\}] \\ & + \widehat{\text{E}}_{\mathcal{LM}_r} \left[ \widehat{r}_{\mathcal{LM}}(\mathbf{X}_{\Omega_r}) h(\mathbf{X}_{\Omega_r}) \{\tilde{\varphi}_{1,r}(\tilde{\boldsymbol{\delta}}_r) - \widehat{m}_r(\mathbf{X}_{\Omega_r})\} \right] \\ & - \widehat{\text{E}}_{\mathcal{LC}} \left[ \widehat{r}_{\mathcal{LC}}(\mathbf{X}_{\Omega_0}) h(\mathbf{X}_{\Omega_r}) \{\tilde{\varphi}_{1,r}(\tilde{\boldsymbol{\delta}}_r) - \widehat{m}_r^*(\mathbf{X}_{\Omega_r})\} \right], \end{aligned} \quad (12)$$

where the second and third terms correct bias of the ML-plugin estimator in the first row.

Based on this, we estimate  $\bar{\Delta}_r$  through:

$$\hat{\Delta}_r = \hat{L}(\hat{h}), \quad \text{where} \quad \hat{h} = \arg \max_{h \in \mathcal{G}} \hat{L}(h). \quad (13)$$

Again, cross-fitting for the ML estimators  $\tilde{\varphi}_{1,r}$  and  $\tilde{\boldsymbol{\delta}}_r$  is required. Asymptotic property of  $\hat{\Delta}_r$  is established in Supplementary Material. This enables consistent identification of misaligned  $\mathcal{LM}_r$  with  $\bar{\Delta}_r \gg \{d(n)/n\}^{1/2}$ , where  $d(n)$  is a model complexity parameter of the model space  $\mathcal{G}$  that may depend on  $n$ ; see Section 3.3 for details. Based on this, we take the well-aligned set as  $\hat{\mathcal{A}} = \{r : \hat{\Delta}_r < \tau\}$ , where the threshold parameter  $\tau = \{d(n)/n\}^{1/2-\epsilon}$  for some small  $\epsilon > 0$ , saying  $\epsilon = 0.02$  in practice. Only those  $\mathcal{LM}_r$  sources with  $r \in \hat{\mathcal{A}}$  will be used for the data fusion in Section 2.2. In practice, one can first obtain  $\hat{\mathcal{A}}$  based on  $\tilde{\varphi}_{1,r}$ 's and  $\tilde{\boldsymbol{\delta}}_r$ 's computed by (8) with all BM sources included, and then update the calibration parameter  $\tilde{\boldsymbol{\delta}}$  by (8) with  $r \in \hat{\mathcal{A}}$  only.

Finally, we consider the general setup without  $\Omega_0 \subseteq \Omega_r$ . In this scenario, the alignment assumption (1) no longer implies  $m_r(\mathbf{x}_{\Omega_r}) = m_r^*(\mathbf{x}_{\Omega_r})$ . Instead, we introduce

$$m_r^{**}(\mathbf{x}_{\Omega_r}) := E_{UC} \left\{ E_{\mathcal{LC}} [\tilde{\varphi}_{1,r}(\mathbf{X}_{\Gamma_r}, Y, \tilde{\boldsymbol{\delta}}_r) \mid \mathbf{X}_{\Omega_0 \cup \Omega_r}, \tilde{\varphi}_{1,r}, \tilde{\boldsymbol{\delta}}_r] \mid \mathbf{X}_{\Omega_r} \right\}.$$

It is not hard to show that both  $m_r^{**}(\mathbf{x}_{\Omega_r})$  and  $m_r(\mathbf{x}_{\Omega_r})$  are equal to  $E_{UC} [\tilde{\varphi}_{1,r}(\mathbf{X}_{\Gamma_r}, Y, \tilde{\boldsymbol{\delta}}_r) \mid \mathbf{X}_{\Omega_r}, \tilde{\varphi}_{1,r}, \tilde{\boldsymbol{\delta}}_r]$  when (1) holds for  $\mathcal{LM}_r$ . Thus, we define  $\bar{\Delta}_r$  in this scenario by replacing  $m_r^*$  with  $m_r^{**}$  in  $L(h)$  of equation (11). Empirically,  $m_r^{**}(\mathbf{x}_{\Omega_r})$  can be estimated by first regressing  $\tilde{\varphi}_{1,r}(\mathbf{X}_{\Gamma_r}, Y, \tilde{\boldsymbol{\delta}}_r)$  against  $\mathbf{X}_{\Omega_0 \cup \Omega_r}$  on  $\mathcal{LC}$  and then integrating the estimator over  $p_{UC}(\mathbf{X}_{\Omega_0 \cup \Omega_r} \mid \mathbf{X}_{\Omega_r})$  or regressing it against  $\mathbf{X}_{\Omega_r}$  with the  $UC$  data. Again, to avoid overfitting bias, we require cross-fitting of all nuisance ML models, including the DML operators, control functions, and calibration functions.

## 3 Asymptotic Analysis

### 3.1 Asymptotic properties of DEFUSE

In this section, we establish the asymptotic properties of DEFUSE. We assume that  $\rho_r = n_r/n$  converges to some  $\bar{\rho}_r \in (0, \infty)$ ,  $n + \sum_{r=1}^R n_r = o(N)$ . The main assump-

tions are introduced in Appendix A. In summary, Assumption A1 includes mild regularity conditions on the distribution of the variables, overlapping (positivity) assumption between data sources, and positive definiteness of the hessian matrix. Assumption A2 imposes that the nuisance ML estimators  $\widehat{r}_{\mathcal{L}\mathcal{C}}(\cdot)$ ,  $\widehat{r}_{\mathcal{L}\mathcal{M}}(\cdot)$ ,  $\widehat{E}_{\mathcal{L}\mathcal{C}}[\cdot \mid \mathbf{X}_{\Omega_0}]$  and  $\widehat{E}_{\mathcal{L}\mathcal{M}_r}[\cdot \mid \mathbf{X}_{\Omega_r}]$  converge to the corresponding true functions with their  $L_2$ -errors being  $o_{\mathbb{P}}(n^{-1/4})$ , which is known as the DML or rate doubly robust assumption (Chernozhukov et al., 2016). Assumption A3 imposes the consistency of the empirical control functions  $\widetilde{\phi}_{1,r}$ ,  $\widetilde{\phi}_{2,r}$  and the calibrating parameters  $\widetilde{\boldsymbol{\delta}}$ ,  $\widetilde{\boldsymbol{\zeta}}$ . Importantly, we only require their  $o_{\mathbb{P}}(1)$ -convergence to limiting values or functions denoted as  $\bar{\phi}_{1,r}$ ,  $\bar{\phi}_{2,r}$ ,  $\bar{\boldsymbol{\delta}}$  and  $\bar{\boldsymbol{\zeta}}$ , but *not* necessarily any true conditional models like  $\phi_r^*$ .

**Remark 2.** *Notably, our required convergence rates on the nuisance functions differ substantially between Assumptions A2 and A3. For the density ratio and conditional mean models with the input  $\mathbf{X}_{\Omega_r}$ ,  $o_{\mathbb{P}}(n^{-1/4})$ -convergence to the truth is required such that the DML constructions  $\widehat{\mathfrak{M}}_{\mathcal{L}\mathcal{C}}(\cdot)$ ,  $\widehat{\mathfrak{M}}_{\mathcal{L}\mathcal{M}_r}(\cdot)$  can adjust for distributional shifts and ensure  $n^{1/2}$ -consistency. In contrast, for the control functions and calibrating parameters, we only require a much less stringent  $o_{\mathbb{P}}(1)$  rate, thanks to our DML construction adjusting for distributional shifts of the control variates. This is a blessing for the incorporation of high-dimensional or AI-derived features into the control functions as mentioned in Remark 1.*

Theorems 1 and 2 establish that the DEFUSE estimators  $\widehat{\beta}_1$  and  $\widehat{\beta}_2$  are  $\sqrt{n}$ -consistent, asymptotically unbiased, and asymptotically normal under Assumptions A1–A3. Based on these theorems, the efficiency properties of  $\widehat{\beta}_1$  and  $\widehat{\beta}_2$  are established next.

**Theorem 1** (Convergence of DEFUSE $_{\mathcal{L}\mathcal{M}}$ ). *Under Assumptions A1–A3,  $\widehat{\beta}_1 \xrightarrow{p} \mathbf{c}^\top \bar{\boldsymbol{\gamma}}$  and*

$$\sqrt{n}(\widehat{\beta}_1 - \mathbf{c}^\top \bar{\boldsymbol{\gamma}}) = \sqrt{n}\widehat{E}_{\mathcal{L}\mathcal{C}}[\mathfrak{M}_{\mathcal{L}\mathcal{C}}(\bar{S}_1)] + \sum_{r=1}^R \sqrt{n}\widehat{E}_{\mathcal{L}\mathcal{M}_r}[\mathfrak{M}_{\mathcal{L}\mathcal{M}_r}(\bar{\varphi}_{1,r}(\bar{\boldsymbol{\delta}}_r))] + o_{\mathbb{P}}(1),$$

where  $\bar{S}_1 = \mathbf{c}^\top \bar{\mathbf{S}} - \sum_{r=1}^R \bar{\varphi}_{1,r}(\bar{\boldsymbol{\delta}}_r)$  and  $\bar{\varphi}_{1,r}(\boldsymbol{\delta}_r) = \bar{\phi}_{1,r}(\mathbf{X}_{\Gamma_r}, Y)w_r(\mathbf{Z}_r; \boldsymbol{\delta}_r)$ . Consequently,  $\sqrt{n}(\widehat{\beta}_1 - \mathbf{c}^\top \bar{\boldsymbol{\gamma}})$  weakly converges to some normal distribution with mean zero.

**Theorem 2** (Convergence of DEFUSE). *Under Assumptions A1–A3,  $\widehat{\beta}_2 \xrightarrow{p} \mathbf{c}^\top \widetilde{\gamma}$  and*

$$\sqrt{n}(\widehat{\beta}_2 - \mathbf{c}^\top \widetilde{\gamma}) = \sqrt{n} \widehat{\mathbb{E}}_{\mathcal{L}\mathcal{C}} [\mathfrak{M}_{\mathcal{L}\mathcal{C}}(\bar{S}_1 - \bar{\varphi}_2(\bar{\boldsymbol{\zeta}}))] + \sum_{r=1}^R \sqrt{n} \widehat{\mathbb{E}}_{\mathcal{L}\mathcal{M}_r} [\mathfrak{M}_{\mathcal{L}\mathcal{M}_r}(\bar{\varphi}_{1,r}(\bar{\boldsymbol{\delta}}_r))] + o_p(1),$$

where  $\bar{\varphi}_2(\boldsymbol{\zeta}) = \bar{\phi}_2(\mathbf{X})h(\mathbf{X}; \boldsymbol{\zeta})$ . Also,  $\sqrt{n}(\widehat{\beta}_2 - \mathbf{c}^\top \widetilde{\gamma})$  weakly converges to normal distribution with mean zero.

## 3.2 Efficiency Properties

In this section, we justify the intrinsic efficiency of DEFUSE and study its relative efficiency (RE) compared to a broad range of approaches, including the  $\mathcal{L}\mathcal{C}$ -only estimator, existing methods for BM regression (e.g., Miao et al., 2023; Wang et al., 2023), SS methods that incorporate only the  $\mathcal{U}\mathcal{C}$  sample (e.g., Chakraborty and Cai, 2018). Define  $RE(\widehat{b}_1|\widehat{b}_2) = AVar(\widehat{b}_2)/AVar(\widehat{b}_1)$  as the RE between two asymptotically normal estimators  $\widehat{b}_1$  and  $\widehat{b}_2$ , where  $AVar(\cdot)$  represents their asymptotic variances. We start with the task of combining  $\mathcal{L}\mathcal{C}$  with  $\mathcal{L}\mathcal{M}$ , and establish the relative efficiency of  $DEFUSE_{\mathcal{L}\mathcal{M}}$  to the  $\mathcal{L}\mathcal{C}$ -only estimator  $\mathbf{c}^\top \widetilde{\gamma}$  and the estimator  $\beta^\dagger$  defined in (6) without calibration.

**Corollary 1** (Intrinsic Efficiency and Adaptivity). *Under Assumptions A1–A3,  $\widehat{\beta}_1 \equiv \widehat{\beta}_1(\widetilde{\boldsymbol{\delta}})$  is intrinsically efficient, i.e., having the smallest asymptotic variance being  $\min_{\boldsymbol{\delta} \in \mathcal{C}_\delta} \bar{Q}(\boldsymbol{\delta})$ , among the class of estimators  $\{\widehat{\beta}_1(\boldsymbol{\delta}) : \boldsymbol{\delta} \in \mathcal{C}_\delta\}$  defined in (7), where*

$$\bar{Q}(\boldsymbol{\delta}) = \text{Var}_{\mathcal{L}\mathcal{C}} \left[ \mathfrak{M}_{\mathcal{L}\mathcal{C}} \left( \mathbf{c}^\top \bar{S} - \sum_{r=1}^R \bar{\varphi}_{1,r}(\boldsymbol{\delta}_r) \right) \right] + \sum_{r=1}^R \frac{1}{\rho_r} \text{Var}_{\mathcal{L}\mathcal{M}_r} [\mathfrak{M}_{\mathcal{L}\mathcal{M}_r}(\bar{\varphi}_{1,r}(\boldsymbol{\delta}_r))].$$

Consequently, when Assumption A4 further holds,  $RE(\widehat{\beta}_1|\mathbf{c}^\top \widetilde{\gamma}) \geq 1$  and  $RE(\widehat{\beta}_1|\beta^\dagger) \geq 1$ .

**Remark 3.** *Assumption A4 used in Corollary 1 assumes that constants 1 and 0 belong to feasible sets of our calibration functions. This is not hard to realize by our Examples 1–3. Essentially, it ensures that both the  $\mathcal{L}\mathcal{C}$ -only estimator  $\mathbf{c}^\top \widetilde{\gamma}$  and the uncalibrated  $\beta^\dagger$  belong to  $\{\widehat{\beta}_1(\boldsymbol{\delta}) : \boldsymbol{\delta} \in \mathcal{C}_\delta\}$ , ensuring the adaptivity of  $DEFUSE_{\mathcal{L}\mathcal{M}}$  in the sense that  $AVar(\widehat{\beta}_1) \leq AVar(\mathbf{c}^\top \widetilde{\gamma})$  and  $AVar(\widehat{\beta}_1) \leq AVar(\beta^\dagger)$ , even when the control function  $\bar{\varphi}_{1,r}$  is of low quality or the BM data is not informative.*

Note that  $\widehat{\beta}_1$  generally does not achieve semiparametric efficiency, which is computationally challenging in non-monotonically missing settings like ours. Instead of pursuing semiparametric efficiency, our method is computationally more feasible and tractable, especially when integrating complex ML methods. This is because calculating the efficient influence function for non-monotone missingness requires recursively updating multiple ML models, leading to high computational costs and convergence issues.

In Corollary 2, we quantify the efficiency gain obtained by incorporating the  $\mathcal{UC}$  sample to further improve the efficiency of  $\widehat{\beta}_1$  as described in Section 2.3. Building on this, all the above corollaries and remarks regarding  $\widehat{\beta}_1$  naturally extend to our final estimator  $\widehat{\beta}_2$ .

**Corollary 2** (Gain of SSL). *Under Assumptions A1–A4,  $RE(\widehat{\beta}_2|\widehat{\beta}_1) = \bar{T}(\mathbf{0})/\min_{\boldsymbol{\zeta}} \bar{T}(\boldsymbol{\zeta}) \geq 1$ , where  $\bar{T}(\boldsymbol{\zeta}) = \text{Var}_{\mathcal{LC}} [\bar{\mathfrak{M}}_{\mathcal{LC}}(\bar{S}_1(\mathbf{X}, Y) - \bar{\varphi}_2(\boldsymbol{\zeta}))] + \sum_{r=1}^R \bar{\rho}_r^{-1} \text{Var}_{\mathcal{LM}_r} [\mathfrak{M}_{\mathcal{LM}_r}(\bar{\varphi}_{1,r}(\bar{\boldsymbol{\delta}}_r))]$ , with a strict  $>$  holding when the correlation of  $\bar{S}_1(\mathbf{X}, Y)$  and  $\bar{\varphi}_2(\bar{\boldsymbol{\zeta}})$  is not zero.*

The efficiency improvement of the SS estimator  $\widehat{\beta}_2$  over  $\widehat{\beta}_1$ , as stated in Corollary 2, has not been previously achieved by existing work also considering the SS and BM setting (Xue et al., 2021; Song et al., 2024). Furthermore, Corollary 2 implies that DEFUSE outperforms the SS estimator of Chakraborty and Cai (2018), which is shown to be optimal under the standard MCAR and SS setting involving only  $\mathcal{LC}$  and  $\mathcal{UC}$ .

### 3.3 Screening Misaligned Sources

In this section, we study the theoretical property of the screening method introduced in Section 2.4. We introduce two additional assumptions. Assumption A5 imposes that the complexity of the function class  $\mathcal{G}$  used in (11) is controlled by some effective dimensionality parameter  $d(n)$ , which is commonly used for studying the empirical process in learning theory (e.g., Van Der Vaart and Wellner, 1996). Assumption A6 requires the misaligned sources indexed by  $\mathcal{A}^c$  exhibit sufficiently large discrepancy from the benchmark  $\mathcal{LC}$ , specifically, the root MSD  $\bar{\Delta}_r = O_{\mathbb{P}}(\{d(n)/n\}^{1/2-c})$  with some  $c > 0$ , for all  $r \in \mathcal{A}^c$ . This ensures that the aligned BM sources ( $\bar{\Delta}_r = 0$ ) and the misaligned ones ( $\bar{\Delta}_r > 0$ ) can be well-separated by a proper threshold on  $\bar{\Delta}_r$ . Theorem 3 shows that our screening method can correctly exclude them while preserving the aligned ones, with probability approaching one. Consequently, our pipeline is “oracle” in the sense that the estimator constructed using the

screened BM sources in  $\widehat{\mathcal{A}}$  is asymptotically equivalent to the ideal one obtained with the knowledge of true  $\mathcal{A}$ .

**Theorem 3** (Selection consistency for aligned sources). *Under Assumptions A1–A3, A5, A6 and assuming  $h_r^*(\mathbf{x}_{\Omega_r}) := \{m_r(\mathbf{x}_{\Omega_r}) - m_r^*(\mathbf{x}_{\Omega_r})\} / \{\mathbf{E}_{\mathcal{UC}}[m_r(\mathbf{x}_{\Omega_r}) - m_r^*(\mathbf{x}_{\Omega_r})]^2\}^{1/2} \in \mathcal{G}$  for all  $r \in \mathcal{A}^c$ , there exists  $\epsilon > 0$  such that screening set  $\widehat{\mathcal{A}} = \{r : \widehat{\Delta}_r < \{d(n)/n\}^{1/2-\epsilon}\}$  is consistent with the true  $\mathcal{A} := \{r : \bar{\Delta}_r = 0\}$ , i.e.,  $\Pr(\widehat{\mathcal{A}} = \mathcal{A}) \rightarrow 1$  as  $n \rightarrow \infty$ .*

**Remark 4.** *Theorem 3 considers a simplified setup directly assuming the truth  $h_r^* \in \mathcal{G}$ . For methods like kernel regression,  $\mathcal{G}$  used in (13) does not exactly contain  $h_r^*(\cdot)$  but approximates it as  $n \rightarrow \infty$ . Our analyses can be generalized to such scenarios. When the sample sizes are relatively small, one may choose  $\mathcal{G}$  in (13) with low complexity (e.g., low-dimensional parametric models) for the sake of bias-variance tradeoff, even though it may be misspecified. Meanwhile, the commonly used mean-difference strategy (e.g., Cheng and Cai, 2021; Miao et al., 2023; Han et al., 2025) actually corresponds to setting the function space  $\mathcal{G} = \{1\}$  in our framework, which may be too simple to capture the misalignment compared to a more properly specified  $\mathcal{G}$  in our method.*

**Remark 5.** *The consistency in Theorem 3 may not hold when there exist misaligned sources with  $\bar{\Delta}_r \asymp \{d(n)/n\}^{1/2}$  contradicting Assumption A6. In the presence of misaligned sources with insufficient discrepancy for detection, our framework cannot ensure valid, asymptotically normal inference while fusing all aligned sources. A similar impossibility result was established in Chen et al. (2025) on the fusion of experimental and observational studies. Rigorously justifying this in our setting warrants future study. To mitigate this, one may incorporate non-normal inference approaches (Yang and Ding, 2019; Guo et al., 2025).*

## 4 Simulation Study

We conduct simulation studies to assess the performance of DEFUSE, in comparison with a broad range of existing methods. Table 1 summarizes all simulation settings including various data generation and missing mechanisms. Specifically, we distinguish between the MCAR and MAR mechanisms and consider both the binary and continuous response scenarios. We also include the single BM ( $R = 1$ ) and multiple BM ( $R > 1$ ) settings, and

study the impact of dimensionality and nonlinear effects in the models for the missing covariates and the outcome. Detailed data-generating processes are provided in Supplementary Material.

Setting	(I)	(II)	(III)	(IV)	(V)	(VI)
Missing Mechanism	MCAR	MCAR	MCAR	MAR	Misaligned	MAR
Number of $R$	1	1	2	1,2	4	1
Response Type	Continuous	Binary	Continuous	Continuous	Continuous	Continuous
$\mathbf{X}_{\Gamma_r} \mathbf{X}_{\Gamma}$	Linear	Nonlinear	Linear	Linear	Linear	Linear
$Y \mathbf{X}$	Linear	–	Linear	Nonlinear	Nonlinear	Linear
High-dimensional $\mathbf{X}$	–	–	–	–	–	Yes

Table 1: **Summary of simulation setups.** Each column (I)–(VI) represents a distinct simulation setting varying by missing mechanisms (MCAR, MAR, presence of Misaligned sources), response type (continuous or binary), number of sources  $R$ , and model structure. “Linear/Nonlinear” indicates whether nonlinear effects are included in the generating mechanism or not.

We summarize methods under comparison as below.  **$\mathcal{LC}$ -only:** The preliminary estimator  $\tilde{\gamma}$ .  **$\text{DEFUSE}_{\mathcal{LM}}$ :**  $\hat{\beta}_1$  obtained using  $\mathcal{LC}$  and  $\mathcal{LM}_r$  sources as introduced in Section 2.2.  **$\text{DEFUSE}$ :**  $\hat{\beta}_2$  obtained by further using the SS method in Section 2.3. For our method, we include different versions of calibration and control functions. The suffixes **Eg 1** and **Eg 2** indicate constant and linear calibration schemes described in Examples 1 and 2. The suffixes **CM** and **RM** denote different control variate strategies discussed in Section 3.2, where **CM** represents our proposed conditional mean model and **RM** corresponds to the reduced working model strategy in a spirit similar to (e.g., Wang et al., 2023). **MICE:** Multiple imputation by chained equations (van Buuren and Groothuis-Oudshoorn, 2011). **MBI:** The multiple blockwise imputation method (Xue and Qu, 2021) combining  $\mathcal{LC}$  and  $\mathcal{LM}$  data. **HTLGMM:** The data fusion approach (Zhao et al., 2023) based on the generalized method of moments. **SC:** the approach (Wang et al., 2023) using Sample-reweighting for Calibration of the target model. SC and HTLGMM are built upon the same reduced working parametric model of  $Y \sim \mathbf{X}_{\Gamma_r}$ . Although constructed in different ways, they actually have the same asymptotic variance in the MCAR setting. In MAR settings, we also include **SC-PW**, a straightforward extension of SC used in Wang et al. (2023) that leverages  $\hat{r}_{\mathcal{LC}}$  and  $\hat{r}_{\mathcal{LM}_r}$  as propensity weights to adjust for distributional shifts between sources. **SSB:** The SS and BM fusion method proposed by (Song et al., 2024) using the  $\mathcal{LC}$ ,  $\mathcal{LM}$  and  $\mathcal{UC}$

samples. **Class.Semi.Eff:** The classic semiparametric efficient estimator (Robins et al., 1994) optimal under the MCAR scenario with  $R = 1$ . **SSL:** The SS estimator using  $\mathcal{LC}$  and  $\mathcal{UC}$  (e.g., Gronsbell et al., 2022).

In Setting (I), we assess estimator performance across  $\rho \equiv \rho_1 \in 2, 3, 4, 5$ . Supplementary Table S1 reports the average relative efficiency (RE) against the  $\mathcal{LC}$ -only estimator, computed as the inverse of the mean squared error averaged over all target coefficients and the mean absolute bias. All estimators, except MICE, exhibit small biases. Our DEFUSE consistently outperforms other methods in RE. For example, it achieves roughly 20% higher RE than HTLGMM, MBI and SC at  $\rho = 2$ , with larger gains as  $\rho$  increases. Since the conditional model is correctly specified,  $\text{DEFUSE}_{\mathcal{LM}}$  has almost the same performance to the classic semiparametric efficient estimator (Class.Semi.Eff). And the linear calibration further improves the performance of  $\text{DEFUSE}_{\mathcal{LM}}$  compared with constant calibration.

For Settings (II) and (III), we present component-wise RE to  $\mathcal{LC}$ -only in Table 2. In terms of fusing  $\mathcal{LC}$  and  $\mathcal{LM}_r$ 's,  $\text{DEFUSE}_{\mathcal{LM}}$  consistently attains higher efficiency than MBI, SSB, HTLGMM, and SC. It shows about 50% higher RE on  $\gamma_1$  compared with SSB and MBI, while standard SSL method provides little to no gain when the outcome model is correct. When the conditional model for missing covariates is misspecified as Setting (II), we compare two calibration schemes Examples (Egs) 1 and 2. Eg 1 based on constant calibration shows lower efficiency than Eg 2 involving parametric calibration models. For instance,  $\text{DEFUSE}_{\mathcal{LM}}$  with Eg 2 attains about 40% higher RE on  $\gamma_3$  than Eg 1, highlighting the advantage of our data-adaptive and intrinsic efficient calibration framework.

In the MAR Setting (IV), we vary three key factors: the degree of distributional shift, the strength of nonlinear effects, and the number of missing blocks. As shown in Table 3,  $\mathcal{LC}$ -only,  $\text{DEFUSE}_{\mathcal{LM}}$ , and DEFUSE exhibit substantially small mean absolute biases relative to their standard errors and their biases remain relatively stable when the degree of density shift or nonlinearity increases. In contrast, SC-PW and MBI encounter excessive bias. For example, when  $R = 1$  and shift = 0.1, SC-PW yields a bias of 0.234 that is times higher than DEFUSE. This is due to the ML errors of the nuisance model and demonstrates the necessity of DML when using ML nuisance estimators.  $\text{DEFUSE}_{\mathcal{LM}}$  with our CM strategy attains higher RE than RM, its reduced working model counterpart. For example, when  $R = 1$  and shift = 0.3, CM reaches RE = 1.54, compared to RM's RE = 1.14.

Method	Setting (II)					Setting (III)				
	$\gamma_1$	$\gamma_2$	$\gamma_3$	$\gamma_4$	$\gamma_5$	$\gamma_1$	$\gamma_2$	$\gamma_3$	$\gamma_4$	$\gamma_5$
Class.Semi.Eff	4.48	3.84	2.86	0.99	1.00	-	-	-	-	-
DEFUSE $_{\mathcal{LM}}$ Eg 1	4.44	3.99	3.12	0.98	0.96	1.60	1.78	2.39	1.49	1.67
DEFUSE $_{\mathcal{LM}}$ Eg 2	4.87	5.11	3.90	1.23	1.06	-	-	-	-	-
MICE	4.86	10.01	4.92	0.18	0.58	0.52	0.63	0.69	0.20	0.22
MBI	-	-	-	-	-	1.06	1.09	1.06	0.95	1.01
SSL	1.01	1.08	1.00	0.93	1.25	1.01	1.00	1.00	0.99	1.02
SSB	-	-	-	-	-	1.07	1.12	1.51	0.60	0.81
HTLGMM	2.41	2.80	1.90	1.06	1.09	-	-	-	-	-
SC	2.43	2.79	1.91	1.07	1.10	-	-	-	-	-

Table 2: Relative efficiency (RE) to  $\mathcal{LC}$ -only on each coefficient in Settings (II) and (III).

Also, the RE of DEFUSE $_{\mathcal{LM}}$  increases with the degree of distributional shift, rising from approximately 1.24 to above 1.54. Importantly, DEFUSE shows 20%–40% efficiency gain over DEFUSE $_{\mathcal{LM}}$ , demonstrating the benefit of our SS method in Section 2.3. Similar results hold for the case with  $R > 1$  in Setting (IV).

Setting (VI) further investigates the MAR scenario with high-dimensional auxiliary features in  $\mathbf{X}$ , where we vary both the number of features in the sufficient alignment set  $\Omega_r$  and the number of the other features. Our design also mimics posthoc features frequently used in EMR studies. The results are summarized in Table 4. DEFUSE $_{\mathcal{LM}}$  consistently exhibit small absolute biases and achieve substantial efficiency gains compared to the  $\mathcal{LC}$ -only baseline and DEFUSE shows significantly improved efficiency over DEFUSE $_{\mathcal{LM}}$  again.

In Setting (V) with misaligned sources violating the MAR assumption, we evaluate the screening performance of our screening approach based on the mean squared difference (MSD)  $\bar{\Delta}_r^2$  introduced in Section 2.4, across varying degrees of distributional shifts and number of misaligned sources. Our performance metrics include the area under the receiver operating characteristic curve (AUC) and F1 score for discerning the misaligned sources from the aligned ones. In Figure 1, we present the AUC and F1 score of our method as well as the commonly used mean difference (MD) strategy discussed in Remark 4. For fair comparison, both methods incorporate debiasing. Our strategy attains AUC and F1 score close to 1 in all cases while MD fails to provide consistent selection of the misaligned sources. This result agrees with our theoretical conclusion and discussion in Section 3.3.

$R$	<b>Bias<sub>SE</sub></b>	<b>Degree of Density Shift</b>			<b>Nonlinearity</b>		
		0.1	0.2	0.3	0.25	0.50	0.75
$R = 1$	$\mathcal{LC}$ -only	0.023 <sub>0.118</sub>	0.033 <sub>0.147</sub>	0.043 <sub>0.210</sub>	0.022 <sub>0.119</sub>	0.033 <sub>0.147</sub>	0.033 <sub>0.184</sub>
	DEFUSE $_{\mathcal{LM}}$ CM	0.021 <sub>0.106</sub>	0.031 <sub>0.127</sub>	0.040 <sub>0.169</sub>	0.016 <sub>0.103</sub>	0.031 <sub>0.127</sub>	0.045 <sub>0.159</sub>
	DEFUSE $_{\mathcal{LM}}$ RM	0.023 <sub>0.116</sub>	0.030 <sub>0.141</sub>	0.038 <sub>0.197</sub>	0.022 <sub>0.115</sub>	0.030 <sub>0.141</sub>	0.039 <sub>0.176</sub>
	DEFUSE CM	0.028 <sub>0.098</sub>	0.038 <sub>0.113</sub>	0.052 <sub>0.145</sub>	0.020 <sub>0.093</sub>	0.038 <sub>0.113</sub>	0.056 <sub>0.141</sub>
	MBI	0.125 <sub>0.159</sub>	0.222 <sub>0.246</sub>	0.281 <sub>0.301</sub>	0.098 <sub>0.122</sub>	0.222 <sub>0.246</sub>	0.344 <sub>0.377</sub>
	SC-PW	0.234 <sub>0.271</sub>	0.408 <sub>0.435</sub>	0.529 <sub>0.551</sub>	0.198 <sub>0.220</sub>	0.408 <sub>0.425</sub>	0.628 <sub>0.663</sub>
	<b>RE</b>	0.1	0.2	0.3	0.25	0.50	0.75
$R = 1$	DEFUSE $_{\mathcal{LM}}$ CM	1.24	1.34	1.54	1.34	1.34	1.34
	DEFUSE $_{\mathcal{LM}}$ RM	1.04	1.08	1.14	1.07	1.08	1.09
	DEFUSE CM	1.46	1.68	2.11	1.63	1.68	1.69

Table 3: Mean absolute Bias and RE to the  $\mathcal{LC}$ -only estimator under Setting (IV).

<b>Bias<sub>SE</sub></b>	<b>Number of <math>X_{\Omega_r}</math></b>			<b>Number of <math>X_{\Gamma_r}</math></b>		
	2	4	6	12	22	32
$\mathcal{LC}$ -only	0.010 <sub>0.177</sub>	0.032 <sub>0.206</sub>	0.022 <sub>0.199</sub>	0.011 <sub>0.175</sub>	0.032 <sub>0.206</sub>	0.018 <sub>0.176</sub>
DEFUSE $_{\mathcal{LM}}$ CM	0.015 <sub>0.152</sub>	0.033 <sub>0.164</sub>	0.024 <sub>0.152</sub>	0.016 <sub>0.152</sub>	0.033 <sub>0.164</sub>	0.018 <sub>0.151</sub>
DEFUSE CM	0.009 <sub>0.134</sub>	0.042 <sub>0.130</sub>	0.021 <sub>0.130</sub>	0.014 <sub>0.138</sub>	0.042 <sub>0.130</sub>	0.017 <sub>0.135</sub>
<b>RE</b>	2	4	6	12	22	32
DEFUSE $_{\mathcal{LM}}$ CM	1.36	1.59	1.78	1.34	1.59	1.37
DEFUSE CM	1.75	2.55	2.49	1.61	2.55	1.70

Table 4: Mean absolute Bias and RE to the  $\mathcal{LC}$ -only estimator under Setting (VI).

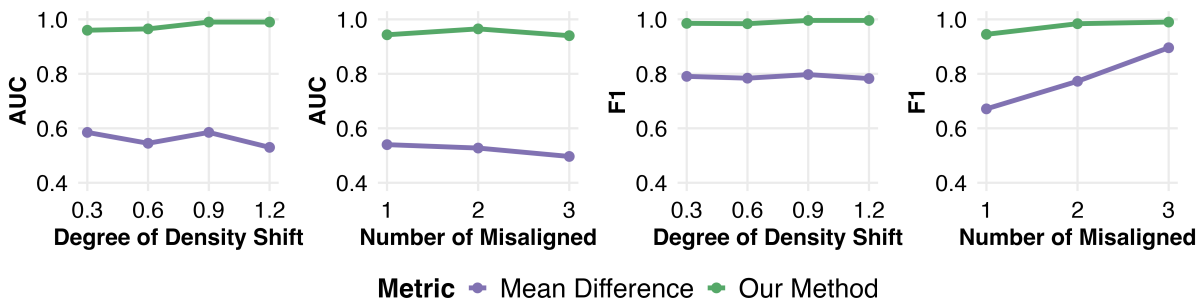


Figure 1: AUC and F1 score in identifying misaligned data sources under Setting (V).

## 5 Real Examples

### 5.1 Alzheimer’s Risk Modeling with NACC data

We apply DEFUSE to the National Alzheimer’s Coordinating Center (NACC) database (Weintraub et al., 2018), a longitudinal cohort compiled from multiple U.S. Alzheimer’s Disease Research Centers, to build a prognostic model for Alzheimer’s disease (AD). The binary outcome  $Y \in \{0, 1\}$  indicates cognitive impairment, and covariates  $\mathbf{X}$  include demographics (gender, race, age, weight, height), behavioral factors (living situation, alcohol use, smoking), and a clinician-assessed language function score (Sonty et al., 2003). Eight centers with missing language scores are initially included, among which three are excluded by our screening method in Section 2.4 due to potential misalignment.

Table 5 presents the relative efficiency (RE) of DEFUSE (Examples 1 and 2) compared with the  $\mathcal{LC}$ -only baseline. DEFUSE $_{\mathcal{LM}}$  with linear calibrating function (Eg 2) consistently outperforms  $\mathcal{LC}$ -only and DEFUSE $_{\mathcal{LM}}$  Eg 1. Also, DEFUSE incorporating unlabeled sample  $\mathcal{UC}$  can further improve RE over DEFUSE $_{\mathcal{LM}}$ , demonstrating the importance of our SS method. For example, for the effect of *Smoke*, DEFUSE Eg 2 achieves an RE of 1.30, around 24% higher than its Eg 1 counterpart using simple allocation for calibration, and 23% higher than DEFUSE $_{\mathcal{LM}}$  Eg 2. Similar improvements are observed for other fully observed covariates, while gains for the partially missing *Language* score is not significant.

Method	Sex	Race	Age	Weight	Height	Life	Alcohol	Smoke	Language
DEFUSE $_{\mathcal{LM}}$ Eg 1	1.09	1.11	1.03	1.00	1.06	1.09	1.00	1.04	1.00
DEFUSE Eg 1	1.17	1.28	1.05	1.01	1.10	1.11	1.04	1.05	1.01
DEFUSE $_{\mathcal{LM}}$ Eg 2	1.13	1.22	1.08	1.07	1.14	1.18	1.02	1.06	1.00
DEFUSE Eg 2	<b>1.19</b>	<b>1.74</b>	<b>1.17</b>	<b>1.14</b>	<b>1.26</b>	<b>1.24</b>	<b>1.11</b>	<b>1.30</b>	<b>1.03</b>

Table 5: Relative efficiency (RE) to the  $\mathcal{LC}$ -only estimator on NACC data.

### 5.2 Heart Disease Risk Modeling with MIMIC-III data

We apply DEFUSE to the MIMIC-III dataset (Johnson et al., 2016) for heart disease (HD) risk modeling, where  $Y \in \{0, 1\}$  denotes HD status determined by manual chart review (Gehrmann et al., 2018). The risk factors  $\mathbf{A}$  include age, low high-density lipoproteins (HDL), type II diabetes, and HD-related laboratory markers, while auxiliary features  $\mathbf{X}$

are derived from diagnostic and procedure codes. We consider two settings: a single BM ( $R = 1$ ) using a composite laboratory risk score (LRS), and a multiple-BM ( $R = 3$ ) case involving two partially missing biomarkers—thyroid-stimulating hormone (TSH) and hypochromia (HPO). All BM sources pass the screening in Section 2.4 under  $\mathbf{X}_{\Omega_r} = \emptyset$ , consistent with the MCAR assumption. Thus, we mainly introduce the MCAR results, with the MAR results included in Supplementary Material.

Table 6 reports the RE of the estimators to the  $\mathcal{L}\mathcal{C}$ -only benchmark. DEFUSE $_{\mathcal{L}\mathcal{M}}$  with both Eg 1 (using simple allocation) and Eg 2 (using linear functions) outperform existing BM data fusion methods. For example, the average RE of DEFUSE $_{\mathcal{L}\mathcal{M}}$  Eg 2 is around 30% higher than those of SC and HTLGMM in the single BM scenario. When our assumption is relaxed to MAR, the RE of DEFUSE to  $\mathcal{L}\mathcal{C}$ -only is still significant and interestingly, the improvement of DEFUSE Eg 2 for calibration over Eg 1 is more significant compared to the MCAR scenario.

Method	Age	HDL	Diabetes	LRS	TSH	Hypochromia
<b>Single BM Scenario</b>						
Class.Semi.Eff	2.14	2.21	2.19	0.98	-	-
DEFUSE $_{\mathcal{L}\mathcal{M}}$ Eg1	2.14	2.21	2.19	1.01	-	-
DEFUSE Eg1	2.15	2.23	2.21	1.01	-	-
DEFUSE $_{\mathcal{L}\mathcal{M}}$ Eg2	2.15	2.21	2.20	1.07	-	-
DEFUSE Eg2	<b>2.16</b>	<b>2.23</b>	<b>2.22</b>	<b>1.11</b>	-	-
SSL	1.07	0.99	1.00	1.00	-	-
HTLGMM	1.76	1.55	1.56	1.02	-	-
SC	1.76	1.55	1.56	1.02	-	-
<b>Multiple BM Scenario</b>						
DEFUSE $_{\mathcal{L}\mathcal{M}}$ Eg1	2.59	1.26	1.28	-	2.00	1.28
DEFUSE Eg1	2.61	1.26	1.29	-	2.10	1.29
DEFUSE $_{\mathcal{L}\mathcal{M}}$ Eg2	2.61	1.26	1.28	-	2.01	1.28
DEFUSE Eg2	<b>2.65</b>	<b>1.29</b>	<b>1.31</b>	-	<b>2.17</b>	<b>1.29</b>
SSL	1.00	0.99	1.06	-	0.94	1.13

Table 6: Relative efficiency (RE) to  $\mathcal{L}\mathcal{C}$ -only estimator in both single BM and multiple BM scenarios on MIMIC-III.

## 6 Discussion

We develop DEFUSE, a novel approach for robust and efficient data fusion in the presence of blockwise missing covariates, large unlabeled samples, and distributional shifts across data sources. Our calibration approach is data-adaptive and robust to arbitrary missing

patterns and model misspecification, remains computationally tractable, and accommodates high-dimensional auxiliary features. Our approach also leverages large unlabeled samples for variance reduction in the SS setting. Furthermore, to tackle source misalignment, we develop a sensitive screening procedure using a debiased MSD measure, which effectively identifies and excludes non-transferable data sources to prevent fusion-induced bias. Theoretical guarantees and extensive experiments confirm DEFUSE’s superiority in maintaining robustness and efficiency, offering a practical and powerful solution for modern data fusion problems.

We shall point out several future directions. Our current method requires the  $\mathcal{LC}$  sample, which may not be accessible in certain scenarios (e.g., Song et al., 2024). Note that (3) can actually be identified and constructed with the  $\mathcal{UC}$  and  $\mathcal{LM}_1, \dots, \mathcal{LM}_R$  samples as long as the union set of the observed covariates in the  $\mathcal{LM}_r$ ’s cover the predictors  $\mathbf{A}$ . It is interesting to generalize our method to accommodate this setting without observation of  $\mathcal{LC}$ . DEFUSE could be generalized to address high-dimensional regression for  $Y \sim \mathbf{A}$ . One can use debiased Lasso (e.g., Van de Geer et al., 2014) to derive the preliminary estimator and base on it to conduct data fusion. Recent work, such as Kundu and Chatterjee (2023), has highlighted the practical need to protect the privacy of individual-level data when fusing datasets collected from different institutions. This need is often addressed by transmitting only summary-level data, e.g., mean vectors and model coefficients (Wolfson et al., 2010).

## References

- Angelopoulos, A. N., Bates, S., Fannjiang, C., Jordan, M. I., and Zrnic, T. (2023a). Prediction-powered inference. *Science*, 382(6671):669–674.
- Angelopoulos, A. N., Duchi, J. C., and Zrnic, T. (2023b). PPI++: Efficient prediction-powered inference. *arXiv preprint arXiv:2311.01453*.
- Aronszajn, N. (1950). Theory of reproducing kernels. *Transactions of the American mathematical society*, 68(3):337–404.
- Castro, V. M., Gainer, V., Wattanasin, N., Benoit, B., Cagan, A., Ghosh, B., Goryachev, S., Metta, R., Park, H., Wang, D., et al. (2022). The mass general brigham biobank portal: an i2b2-based data repository linking disparate and high-dimensional patient data to support multimodal analytics. *Journal of the American Medical Informatics Association*, 29(4):643–651.

- Chakraborty, A. and Cai, T. (2018). Efficient and adaptive linear regression in semi-supervised settings. *The Annals of Statistics*, 46(4):1541–1572.
- Chen, S., Li, S., Zhang, B., and Ye, T. (2025). Minimax rates and adaptivity in combining experimental and observational data. *Journal of Causal Inference*, 13(1):20240024.
- Cheng, D. and Cai, T. (2021). Adaptive combination of randomized and observational data. *arXiv preprint arXiv:2111.15012*.
- Chernozhukov, V., Chetverikov, D., Demirer, M., Dufo, E., Hansen, C., and Newey, W. K. (2016). Double machine learning for treatment and causal parameters. Technical report, cemmap working paper.
- Elliott, J., Bodinier, B., Bond, T. A., Chadeau-Hyam, M., Evangelou, E., Moons, K. G., Dehghan, A., Muller, D. C., Elliott, P., and Tzoulaki, I. (2020). Predictive accuracy of a polygenic risk score-enhanced prediction model vs a clinical risk score for coronary artery disease. *Jama*, 323(7):636–645.
- Gehrmann, S., Deroncourt, F., Li, Y., Carlson, E. T., Wu, J. T., Welt, J., Foote Jr, J., Moseley, E. T., Grant, D. W., Tyler, P. D., et al. (2018). Comparing deep learning and concept extraction based methods for patient phenotyping from clinical narratives. *PloS one*, 13(2):e0192360.
- Glasserman, P. (2004). *Monte Carlo methods in financial engineering*, volume 53. Springer.
- Gretton, A., Smola, A., Huang, J., Schmittfull, M., Borgwardt, K., and Schölkopf, B. (2009). Covariate shift by kernel mean matching. *Dataset shift in machine learning*, 3(4):5.
- Gronsbell, J., Liu, M., Tian, L., and Cai, T. (2022). Efficient evaluation of prediction rules in semi-supervised settings under stratified sampling. *Journal of the Royal Statistical Society: Series B: Statistical Methodology*.
- Guo, Z., Li, X., Han, L., and Cai, T. (2025). Robust inference for federated meta-learning. *Journal of the American Statistical Association*, pages 1–16. Z.G. and X.L. contributed equally to this work.
- Han, L., Hou, J., Cho, K., Duan, R., and Cai, T. (2025). Federated adaptive causal estimation (face) of target treatment effects. *Journal of the American Statistical Association*, (just-accepted):1–25.
- Jin, Y. and Rothenhäusler, D. (2023). Modular regression: Improving linear models by incorporating auxiliary data. *Journal of Machine Learning Research*, 24(351):1–52.
- Johnson, A. E., Pollard, T. J., Shen, L., Lehman, L.-w. H., Feng, M., Ghassemi, M., Moody, B., Szolovits, P., Anthony Celi, L., and Mark, R. G. (2016). MIMIC-III, a freely accessible critical care database. *Scientific data*, 3(1):1–9.
- Kawakita, M. and Kanamori, T. (2013). Semi-supervised learning with density-ratio estimation. *Machine learning*, 91(2):189–209.
- Kundu, P. and Chatterjee, N. (2023). Logistic regression analysis of two-phase studies using generalized method of moments. *Biometrics*, 79(1):241–252.
- Li, S. and Luedtke, A. (2023). Efficient estimation under data fusion. *Biometrika*, 110(4):1041–1054.
- Li, Y., Yang, H., Yu, H., Huang, H., and Shen, Y. (2023). Penalized estimating equations for generalized linear models with multiple imputation. *The Annals of Applied Statistics*, 17(3):2345–2363.
- Liu, M., Zhang, Y., Liao, K. P., and Cai, T. (2023). Augmented transfer regression learning with semi-

- non-parametric nuisance models. *Journal of Machine Learning Research*, 24(293):1–50.
- The All of Us Research Program Investigators (2019). The “all of us” research program. *New England Journal of Medicine*, 381(7):668–676.
- Miao, J., Miao, X., Wu, Y., Zhao, J., and Lu, Q. (2023). Assumption-lean and data-adaptive post-prediction inference. *arXiv preprint arXiv:2311.14220*.
- Qiu, H., Tchetgen Tchetgen, E., and Dobriban, E. (2024). Efficient and multiply robust risk estimation under general forms of dataset shift. *The Annals of Statistics*, 52(4):1796–1824.
- Robins, J. M., Rotnitzky, A., and Zhao, L. P. (1994). Estimation of regression coefficients when some regressors are not always observed. *Journal of the American statistical Association*, 89(427):846–866.
- Rotnitzky, A., Lei, Q., Sued, M., and Robins, J. M. (2012). Improved double-robust estimation in missing data and causal inference models. *Biometrika*, 99(2):439–456.
- Song, S., Lin, Y., and Zhou, Y. (2023). A general m-estimation theory in semi-supervised framework. *Journal of the American Statistical Association*, pages 1–11.
- Song, S., Lin, Y., and Zhou, Y. (2024). Semi-supervised inference for block-wise missing data without imputation. *Journal of Machine Learning Research*, 25(99):1–36.
- Sonty, S. P., Mesulam, M.-M., Thompson, C. K., Johnson, N. A., Weintraub, S., Parrish, T. B., and Gitelman, D. R. (2003). Primary progressive aphasia: Ppa and the language network. *Annals of Neurology: Official Journal of the American Neurological Association and the Child Neurology Society*, 53(1):35–49.
- Tan, Z. (2010). Bounded, efficient and doubly robust estimation with inverse weighting. *Biometrika*, 97(3):661–682.
- van Buuren, S. and Groothuis-Oudshoorn, K. (2011). mice: Multivariate imputation by chained equations in r. *Journal of Statistical Software*, 45(3):1–67.
- Van de Geer, S., Bühlmann, P., Ritov, Y., Dezeure, R., et al. (2014). On asymptotically optimal confidence regions and tests for high-dimensional models. *The Annals of Statistics*, 42(3):1166–1202.
- Van Der Vaart, A. W. and Wellner, J. A. (1996). Weak convergence. In *Weak convergence and empirical processes: with applications to statistics*, pages 16–28. Springer.
- Wang, Z., Kim, H. J., and Kim, J. K. (2023). Survey data integration for regression analysis using model calibration. *Statistics Canada*, 49(1).
- Weintraub, S., Besser, L., Dodge, H. H., Teylan, M., Ferris, S., Goldstein, F. C., Giordani, B., Kramer, J., Loewenstein, D., Marson, D., et al. (2018). Version 3 of the alzheimer disease centers’ neuropsychological test battery in the uniform data set (uds). *Alzheimer Disease & Associated Disorders*, 32(1):10–17.
- Wolfson, M., Wallace, S. E., Masca, N., Rowe, G., Sheehan, N. A., Ferretti, V., LaFlamme, P., Tobin, M. D., Macleod, J., Little, J., et al. (2010). DataSHIELD: resolving a conflict in contemporary bioscience performing a pooled analysis of individual-level data without sharing the data. *International journal of epidemiology*, 39(5):1372–1382.
- Wu, C. and Sitter, R. R. (2001). A model-calibration approach to using complete auxiliary information

- from survey data. *Journal of the American Statistical Association*, 96(453):185–193.
- Wu, D. and Liu, M. (2023). Robust and efficient semi-supervised learning for ising model. *arXiv preprint arXiv:2311.15031*.
- Xue, F., Ma, R., and Li, H. (2021). Statistical inference for high-dimensional linear regression with blockwise missing data. *arXiv preprint arXiv:2106.03344*.
- Xue, F. and Qu, A. (2021). Integrating multisource block-wise missing data in model selection. *Journal of the American Statistical Association*, 116(536):1914–1927.
- Yang, S. and Ding, P. (2019). Combining multiple observational data sources to estimate causal effects. *Journal of the American Statistical Association*.
- Yang, S., Gao, C., Zeng, D., and Wang, X. (2023). Elastic integrative analysis of randomised trial and real-world data for treatment heterogeneity estimation. *Journal of the Royal Statistical Society Series B: Statistical Methodology*, 85(3):575–596.
- Yu, G., Li, Q., Shen, D., and Liu, Y. (2020). Optimal sparse linear prediction for block-missing modality data without imputation. *Journal of the American Statistical Association*, 115(531):1406–1419.
- Zengini, E., Hatzikotoulas, K., Tachmazidou, I., Steinberg, J., Hartwig, F. P., Southam, L., Hackinger, S., Boer, C. G., Styrkarsdottir, U., Gilly, A., et al. (2018). Genome-wide analyses using uk biobank data provide insights into the genetic architecture of osteoarthritis. *Nature genetics*, 50(4):549–558.
- Zhang, Y., Chakraborty, A., and Bradic, J. (2023). Double robust semi-supervised inference for the mean: selection bias under mar labeling with decaying overlap. *Information and Inference: A Journal of the IMA*, 12(3):2066–2159.
- Zhao, R., Kundu, P., Saha, A., and Chatterjee, N. (2023). Heterogeneous transfer learning for building high-dimensional generalized linear models with disparate datasets. *arXiv preprint arXiv:2312.12786*.

## Appendix

### A Assumptions for Theoretical Studies

In this section, we present the assumptions for establishing the asymptotic properties of DEFUSE. Let  $\|\cdot\|_{\mathcal{D},p} = \left\{ \mathbb{E}_{\mathcal{D}}[|\cdot|^p] \right\}^{1/p}$  denote the  $L_p$  norm under the probability measure induced by the data distribution  $\mathcal{D} \in \{\mathcal{LC}, \mathcal{LM}_1, \dots, \mathcal{LM}_R, \mathcal{UC}\}$ . We consider the measurable space  $(\mathcal{X}_{\Omega_r}, \mathcal{B}(\mathcal{X}_{\Omega_r}))$ , where  $\mathcal{X}_{\Omega_r}$  denotes the domain of the covariates in site  $r$  and  $\mathcal{B}(\mathcal{X}_{\Omega_r})$  is the  $\sigma$ -algebra on  $\mathcal{X}_{\Omega_r}$ . Let  $\mathcal{G}$  denote the function class defined in Section 2.4 on  $\mathcal{X}_{\Omega_r}$ . A probability measure  $Q$  on this space is a nonnegative, countably additive set function  $Q : \mathcal{B}(\mathcal{X}_{\Omega_r}) \rightarrow [0, 1]$  satisfying  $Q(\mathcal{X}_{\Omega_r}) = 1$ . Let  $\mathcal{Q}_{\mathcal{X}_{\Omega_r}}$  denote the collection of all

the probability measures on  $\mathcal{X}_{\Omega_r}$ . For any probability measure  $Q \in \mathcal{Q}_{\mathcal{X}_{\Omega_r}}$ , we define the  $L_2(Q)$  of a measurable function  $h : \mathcal{X}_{\Omega_r} \rightarrow \mathbb{R}$  as

$$\|h\|_{L_2(Q)} := \left( \int_{\mathcal{X}_{\Omega_r}} h^2(x) dQ(x) \right)^{1/2}.$$

The  $\epsilon$ -covering number of  $\mathcal{G}$  under the  $L_2(Q)$  metric is defined as

$$N(\mathcal{G}, L_2(Q); \epsilon) = \min \left\{ m : \exists h_1, \dots, h_m \in \mathcal{G}, \forall h \in \mathcal{G}, \min_j \|h - h_j\|_{L_2(Q)} < \epsilon \right\}.$$

We introduce the following collection of outcomes of the ML nuisance regression models:

$$\begin{aligned} D_\gamma &= \mathbf{c}^\top \mathbf{A} \{Y - g(\gamma^\top \mathbf{A})\}, & D_{\phi_{1,r}} &= \phi_{1,r}(\mathbf{X}_{\Gamma_r}, Y), & D_{\phi_2} &= \phi_2(\mathbf{X}), \\ D_{\delta_r} &= \varphi_{1,r}(\mathbf{X}_{\Gamma_r}, Y; \delta_r), & D_\zeta &= \varphi_2(\mathbf{X}; \zeta). \end{aligned}$$

The population calibration parameter  $\bar{\boldsymbol{\delta}}$  and  $\bar{\boldsymbol{\zeta}}$  are defined as the minimizer for the following optimization target:

$$\begin{aligned} \bar{Q}(\boldsymbol{\delta}) &= \text{Var}_{\mathcal{L}\mathcal{C}} \left[ \mathfrak{M}_{\mathcal{L}\mathcal{C}} \left( \mathbf{c}^\top \bar{\mathbf{S}} - \sum_{r=1}^R \bar{\varphi}_{1,r}(\boldsymbol{\delta}_r) \right) \right] + \sum_{r=1}^R \frac{1}{\bar{\rho}_r} \text{Var}_{\mathcal{L}\mathcal{M}_r} \left[ \mathfrak{M}_{\mathcal{L}\mathcal{M}_r}(\bar{\varphi}_{1,r}(\boldsymbol{\delta}_r)) \right], \\ \bar{T}(\boldsymbol{\zeta}) &= \text{Var}_{\mathcal{L}\mathcal{C}} \left[ \bar{\mathfrak{M}}_{\mathcal{L}\mathcal{C}}(\bar{S}_1(\mathbf{X}, Y) - \bar{\varphi}_2(\boldsymbol{\zeta})) \right] + \sum_{r=1}^R \frac{1}{\bar{\rho}_r} \text{Var}_{\mathcal{L}\mathcal{M}_r} \left[ \mathfrak{M}_{\mathcal{L}\mathcal{M}_r}(\bar{\varphi}_{1,r}(\bar{\boldsymbol{\delta}}_r)) \right]. \end{aligned} \tag{A.1}$$

**Assumption A1.** *The derivative of the link function  $g(u)$  is Lipschitz;  $\gamma$  belongs to a compact space including the population-level  $\bar{\gamma}$  as its interior; and the Hessian  $\bar{\mathbf{J}}$  has all its eigenvalues staying away from 0 and  $\infty$ . The density ratio functions  $r_{\mathcal{L}\mathcal{C}}(\mathbf{X}_{\Omega_0})$  and  $r_{\mathcal{L}\mathcal{M}_r}(\mathbf{X}_{\Omega_r})$  are bounded away from 0 and  $\infty$  almost surely and the sample size ratios  $\rho_r$  are away from 0 and  $\infty$ . The joint distribution of  $(Y, \mathbf{A})$  has a continuously differentiable density for the continuous components and satisfies that*

$$\mathbb{E}_{\mathcal{D}} \left[ Y^4 + \|\mathbf{A}\|_2^4 + \{g(\mathbf{A}^\top \bar{\boldsymbol{\gamma}})\}^2 + \{\dot{g}(\mathbf{A}^\top \bar{\boldsymbol{\gamma}})\}^2 \right] < \infty,$$

where  $\mathcal{D} \in \{\mathcal{L}\mathcal{C}, \mathcal{L}\mathcal{M}_1, \dots, \mathcal{L}\mathcal{M}_R, \mathcal{U}\mathcal{C}\}$ .

Under Assumption A1 that  $r_{\mathcal{L}\mathcal{C}}(\cdot)$  and  $r_{\mathcal{L}\mathcal{M}_r}(\cdot)$  stay away from 0 and  $\infty$ , it is not hard to

show that the norms  $\|\cdot\|_{\mathcal{D},p}$  is equivalent for all fixed  $p$  and  $\mathcal{D} \in \{\mathcal{LC}, \mathcal{LM}_1, \dots, \mathcal{LM}_R, \mathcal{UC}\}$ , i.e., there exists some constant  $C > 0$  such that  $C^{-1}\|\cdot\|_{\mathcal{D}_1} \leq \|\cdot\|_{\mathcal{D}_2} \leq C\|\cdot\|_{\mathcal{D}_1}$  for all  $p$  and  $\mathcal{D}_1, \mathcal{D}_2 \in \{\mathcal{LC}, \mathcal{LM}_1, \dots, \mathcal{LM}_R, \mathcal{UC}\}$ . Thus, for the ease of presentation, we use  $\|\cdot\|_p$  to represent the  $L_p$  norm on any  $\mathcal{D} \in \{\mathcal{LC}, \mathcal{LM}_1, \dots, \mathcal{LM}_R, \mathcal{UC}\}$  in the following boundness and rate assumptions.

**Assumption A2.** *The ML nuisance estimators for the density ratio functions satisfies*

$$\left\| \widehat{r}_{\mathcal{LC}}(\mathbf{X}_{\Omega_0}) - r_{\mathcal{LC}}(\mathbf{X}_{\Omega_0}) \right\|_2 + \max_{r \in \{1, \dots, R\}} \left\| \widehat{r}_{\mathcal{LM}_r}(\mathbf{X}_{\Omega_r}) - r_{\mathcal{LM}_r}(\mathbf{X}_{\Omega_r}) \right\|_2 = o_{\mathbb{P}}(n^{-1/4}).$$

For  $D \in \{D_{\bar{\delta}_r}, D_{\delta_r}, D_{\bar{\zeta}}, D_{\zeta}, D_{\bar{\phi}_{1,r}}, D_{\phi_{1,r}}, D_{\bar{\phi}_2}, D_{\phi_2}\}$  and  $D_\gamma$ , the ML nuisance estimators for their conditional mean models satisfy that

$$\begin{aligned} \left\| \widehat{\mathbb{E}}_{\mathcal{LC}}[D \mid \mathbf{X}_{\Omega_0}] - \mathbb{E}_{\mathcal{LC}}[D \mid \mathbf{X}_{\Omega_0}] \right\|_2 &= o_{\mathbb{P}}(n^{-1/4}), \\ \max_{r \in \{1, \dots, R\}} \left\| \widehat{\mathbb{E}}_{\mathcal{LM}_r}[D \mid \mathbf{X}_{\Omega_r}] - \mathbb{E}_{\mathcal{LM}_r}[D \mid \mathbf{X}_{\Omega_r}] \right\|_2 &= o_{\mathbb{P}}(n^{-1/4}), \\ \sup_{\gamma \in \mathcal{N}_n(\bar{\gamma})} \left\| \widehat{\mathbb{E}}_{\mathcal{LC}}[D_\gamma \mid \mathbf{X}_{\Omega_0}] - \mathbb{E}_{\mathcal{LC}}[D_\gamma \mid \mathbf{X}_{\Omega_0}] \right\|_2 &= o_{\mathbb{P}}(n^{-1/4}), \end{aligned}$$

where  $\mathcal{N}_n(\bar{\gamma}) = \{\gamma : \|\gamma - \bar{\gamma}\|_2 \leq s\}$  for some constant  $s > 0$ . In addition, for all  $\mathcal{D} \in \{\mathcal{LC}, \mathcal{LM}_1, \dots, \mathcal{LM}_R, \mathcal{UC}\}$ ,  $\mathbb{E}_{\mathcal{D}}[r_{\mathcal{LC}}^4(\mathbf{X}_{\Omega_0}) + \{\mathbb{E}_{\mathcal{LC}}[D \mid \mathbf{X}_{\Omega_0}]\}^4] < \infty$ .

**Assumption A3.** *For all  $\mathcal{D} \in \{\mathcal{LC}, \mathcal{LM}_1, \dots, \mathcal{LM}_R, \mathcal{UC}\}$ ,  $\mathbb{E}_{\mathcal{D}}(\bar{\varphi}_{1,r}^4 + \phi_{1,r}^4 + \bar{\varphi}_2^4 + \phi_2^4) < \infty$ . There exists some deterministic functions  $\bar{\phi}_{1,r}(\cdot)$  for  $r = 1, \dots, R$  and  $\bar{\phi}_2(\cdot)$  such that*

$$\sum_{r=1}^R \left\| \tilde{\phi}_{1,r}(\mathbf{X}_{\Gamma_r}, Y) - \bar{\phi}_{1,r}(\mathbf{X}_{\Gamma_r}, Y) \right\|_2 = o_{\mathbb{P}}(1), \quad \left\| \tilde{\phi}_2(\mathbf{X}) - \bar{\phi}_2(\mathbf{X}) \right\|_2 = o_{\mathbb{P}}(1).$$

Let  $\bar{\delta}$  and  $\bar{\zeta}$  be the minimizer for the objective functions in (A.1). It is satisfied that

$$\sum_{r=1}^R \left\| w(\mathbf{Z}; \tilde{\delta}_r) - w(\mathbf{Z}; \bar{\delta}_r) \right\|_2 = o_{\mathbb{P}}(1), \quad \left\| h(\mathbf{X}; \tilde{\zeta}) - h(\mathbf{X}; \bar{\zeta}) \right\|_2 = o_{\mathbb{P}}(1).$$

**Assumption A4.** *There exists  $\delta_{0,r}, \delta_{1,r}, \zeta_0, \zeta_1$  belonging to the domain of the calibration functions such that for  $r \in \{1, \dots, R\}$ ,*

$$w(\mathbf{Z}; \delta_{0,r}) = 0, \quad w(\mathbf{Z}; \delta_{1,r}) = 1, \quad h(\mathbf{X}; \zeta_0) = 0, \quad h(\mathbf{X}; \zeta_1) = 1.$$

**Assumption A5.** For any  $r \in \{1, \dots, R\}$ , there exists some  $d(n)$  (that may depend on  $n$ ) and constant  $A > e$  such that for any  $\epsilon > 0$ ,

$$\sup_{Q \in \mathcal{Q}_{\Omega_r}} N(\mathcal{G}, L_2(Q); \epsilon) \leq \left(\frac{A}{\epsilon}\right)^{d(n)}.$$

**Assumption A6.** There exists  $c > 0$  such that for all  $r \in \mathcal{A}^c$ ,  $\bar{\Delta}_r = O_{\mathbb{P}}(\{d(n)/n\}^{1/2-c})$ .

Assumption A5 ensures that the function class  $\mathcal{G}$  used to construct the screening statistics in (13) has controlled complexity, i.e., a VC-type entropy bound. This guarantees that the screening objective  $\widehat{L}(h)$  concentrates around its population counterpart  $L(h)$  in the rate  $O_{\mathbb{P}}(\{d(n)/n\}^{1/2})$ . Assumption A6 requires that the aligned sources ( $r \in \mathcal{A}$ ) and misaligned sources ( $r \in \mathcal{A}^c$ ) exhibit sufficiently different convergence rates in  $\bar{\Delta}_r$ . This ensures that  $\mathcal{A}$  and  $\mathcal{A}^c$  can be well separated, allowing consistent identification of  $\mathcal{A}$ .